# Potential models of quarkonium

A. A. Bykov, I. M. Dremin, and A. V. Leonidov

*P. N. Lebedev Physics Institute, USSR Academy of Sciences*
Usp. Fiz. Nauk **143**, 3–32 (May 1984)

Quarkonia—bound systems of a heavy quark and an antiquark—are described successfully by nonrelativistic potential models. A review is given of the various phenomenological potentials which have been proposed for the interaction of quarks, their application to the description of all the possible characteristics of charmonium and bottomonium, and the corresponding predictions for the hypothetical toponium. The role of relativistic corrections and nonperturbative effects is discussed briefly.

**CONTENTS**

I. Introduction ..... 321
II. Basic information about quarkonia ..... 323
1. Energy levels 2. Decay widths
III. Nonrelativistic potential model ..... 324
1. Assumptions and equations 2. Choice of the interaction potential 3. Theoretical basis
IV. Comparison of the nonrelativistic potential model with experiment ..... 329
1. Comparison of the interaction potentials 2. Energy spectrum 3. Leptonic widths 4. Radiative transitions 5. Total and hadronic widths 6. Predictions for toponium
V. Role of relativistic corrections and possible nonpotential effects ..... 333
1. Relativistic corrections 2. Nonpotential effects
VI. Conclusions ..... 337
Appendix ..... 337
References ..... 337

## I. INTRODUCTION

The acceleration of particles to higher energies has made it possible to advance gradually in the study of truly relativistic effects (for example, processes of multiparticle production). Moreover, paradoxical as it seems, it is at high energies that the particles which can be described theoretically quite well by nonrelativistic quantum mechanics have been found. These are the so-called quarkonia, i.e., the heavy mesons which are regarded as bound states of a heavy quark and an antiquark.[1)]

These particles are of interest primarily because their characteristics can be used to ascertain the nature of their constituent elements, i.e., to study both the static properties of the heavy quarks and the dynamics of their interaction.

From the point of view of the experimentalist, it is possible to obtain quarkonia and investigate their behavior if there exists a suitable (as regards the energy and intensity of the beams) accelerator, although very great ingenuity is required to perform an experiment.

From the point of view of the theoretician, quarkonia also have a number of attractive features. First, they are the simplest two-particle systems consisting of a quark and an antiquark. Second, they are truly bound systems (and not quasibound systems like the ordinary mesons, such as the $\rho$ meson). Third, the quarks in quarkonia move with nonrelativistic velocities. Fourth, the dimensions of quarkonia are so small that one of the basic principles of quantum chromodynamics—asymptotic freedom—must come into play.

Let us explain the foregoing remarks in somewhat greater detail. All the mesons consist of a quark and an antiquark, and the baryons consist of three quarks. The theoretical description of two-particle systems is much simpler than the solution of the three-body problem. Therefore it is natural for theoreticians to tend to occupy themselves at first with mesons, and then to turn to baryons. Of course, it is important in this connection that experiment provides an abundance of information about mesons.

Among all the mesons, quarkonia are considered to be the simplest ones from the point of view of the theoretical understanding of their structure and the dynamics of the interaction of the constituent quarks. The point is that if we consider, for example, the $\rho$ meson as a typical representative of the family of mesons, it can decay into pions in such a way that its constituent quarks remain, as it were, inside the produced pions without changing their character. This decay takes place quite rapidly, after times of the order of the nuclear times. The corresponding quark diagram is shown in Fig. 1a. A decay is possible if the sum of the masses of the newly produced particles is less than the mass of the initial particle. In the case of quarkonia, this condition does not hold for the direct decay channel with conservation of the flavor of their constituent quarks. Quarkonia live much longer than light mesons (i.e., the decay widths of quarkonia

[1)]We recall that quarks of five flavors $u$, $d$, $s$, $c$, and $b$ are now regarded as known, and it is assumed that the $t$ quark exists. The quarks $c$, $b$, and $t$ are said to be heavy (their masses are much greater than 1 GeV).

 0038-5670/84/050321-18$01.80 © 1984 American Institute of Physics 

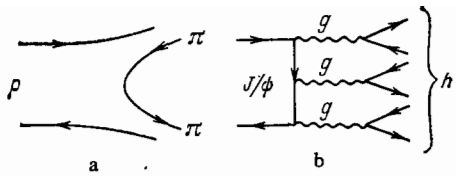


FIG. 1. a) Quark diagram for decay of the $\rho$ meson into two pions; b) quark diagram for decay of the $J/\psi$ into two pions.

are much smaller than those of ordinary mesons) because they are compelled to decay by means of annihilation of a quark and an antiquark, which requires that the latter meet at a single point (Fig. 1b).[2)] Therefore at the hadronic level quarkonia can be regarded as bound systems, unlike the ordinary (quasibound) mesons. A quantitative measure of the binding is the energy which separates a given quarkonium from the threshold for production of the two lightest mesons with the corresponding open flavor.[3)]

The ratio of this energy to the mass of the quarkonium in the ground state provides an approximate (in order of magnitude) estimate of the mean-square velocity of the quarks inside a hadron. It is easy to see that this assertion is correct by making use of the virial theorem and the law of conservation of energy. As will be clear from data on quarkonia presented below, they can be regarded as nonrelativistic quark-antiquark systems, and this simplifies the problem still further.

Finally, quarkonia are very compact systems with dimensions smaller than 1 F (in order of magnitude, the dimensions of quarkonium are determined by $r_Q \sim \alpha_s m_q$, where $\alpha_s \approx 0.2$ is the chromodynamical "constant" and $m_q$ is the quark mass). Thus, their investigation helps us to understand the dynamics of the interaction of quarks at quite small distances.

These attractive features and the promising prospects of the study of quarkonia have brought forth a series of experimental and theoretical investigations of the spectroscopy of quarkonia. As usual, by the term "spectroscopy" we understand here the study of the energy levels of bound systems and all possible transitions between them. The purpose of spectroscopic investigations is to reveal the internal structure of an object and to determine the nature of its constituents and the dynamics of their interaction.

The spectroscopy of the lightest quarkonia is comparatively meager. Moreover, these systems cannot be said to be completely nonrelativistic, since the relativistic corrections for them are still important. With increasing quark mass, there appear more bound states, the relative velocity of the quarks becomes smaller, and the nonrelativistic description becomes better justified.

What can be measured for quarkonia, and what information can be extracted from these measurements?

1. First of all, experimental investigations are made of the *energy levels* of a system. This implies study of the positions of the levels on the scale of energies (the values of the quarkonium masses), their classification (the quantum numbers of the levels), and analysis of the fine and superfine splitting of the levels. From this, information is extracted on the form of the potential in the interval of distances close to the rms radius of the systems as well as other properties of the potential (such as its dependence on the quark flavor), on the behavior of the wave functions at the same distances, and ont the spin-orbit and spin-spin interactions of the constituent quarks.

2. Next, experimental measurements are made of the *total, hadronic and leptonic widths* of quarkonium decays. This gives information about the value of the wave function at zero distance (for $S$ states) or its derivatives (for $P$ and higher states), and also about the electric and color charges of the quarks.

3. Finally, experimental studies are made of *radiative transitions* between the levels of a quarkonium system, i.e., measurements are made of the probabilities (or ratios of the probabilities) of the transitions and their multipolarities. These characteristics provide us with information about the behavior of the wave function at comparatively large distances (exceeding the rms radius) and about the role of relativistic effects in a given system.

Thus, it is in fact possible to ascertain the behavior of the wave function of a system over a rather large interval of distances; this is very important for an understanding of the dynamics of the interaction of quarks.

The theoretical approaches to the description of quarkonia consist of the use of potential models of the sum rules of quantum chromodynamics of lattice models. The first type of approach finds its justification in the nonrelativistic character of quarkonia and is applied to the whole rich set of levels and the transitions between them. The main problem is associated with the choice of the form of the potential (in particular, its spin dependence). In this review, we shall give a detailed account of the results obtained in the framework of the potential approach, and in the individual sections we shall compare them with the results deduced from the sum rules of quantum chromodynamics. The QCD sum rules are more intimately related to the basic principles of the theory of strong interactions, but unfortunately their predictions are in practice limited to the properties of the ground states and do not apply to higher radial excitations. Lattice models have not yet achieved the same predictive power in relation to quarkonia as has been shown by the first two approaches.

Without omitting anything important, we have attempted to make the review as brief as possible, suggesting that the reader who is interested in any particular problem refer to the original papers. We have retained only material which is used directly in calculations based on potential models. In this respect, we have been assisted by earlier reviews of heavy quarks, a list of which is given at the end of the cited literature[58–64] (see also Refs. 2, 4, 6, 18, and 44).

In addition, a large quantity of concrete data on quarkonia is contained in the proceedings of numerous conferences on high-energy physics.

The plan of the review is as follows. After a brief exposition of the experimental data on quarkonia, we turn to an account of potential models and their applications to the

[2)]As we say, they violate the OZI (Okubo-Zweig-Iizuka) rule, and the decays proceed through channels forbidden by this rule.

[3)]We recall that, for example, the system $c\bar{c}$ is a system with open flavor.

spectroscopy of quarkonia. Consideration of the main difficulties which arise when the theory is compared with experiment necessarily leads us to a discussion of the ways in which one might hope to resolve these problems. The prospects which are opening up here seem to us very reassuring, since they provide an opportunity to make use of quarkonia to understand, at least in part, the distinctive character of the dynamics of the interaction of very unusual objects—the quarks.

## II. BASIC INFORMATION ABOUT QUARKONIA

### 1. Energy levels

About ten years ago, in 1974, the discovery was made of charmonium—quarkonium with hidden charm (i.e., the $c\bar{c}$ system). It is denoted by $J/\psi$. Shortly afterwards, its first radially excited state $\psi'$ ws also found, and this was followed by the discovery of quasibound states which decayed into $D$ ($c\bar{u}$, $c\bar{d}$) and $\bar{D}$ mesons. The observation of particles with open charm (first the $D$ mesons in 1976, and then the $F$ mesons with the quark composition $c\bar{s}$) gave definitive confirmation of the hypothesis that charmonium is composed of quarks. The scheme of the energy levels of the charmonium family is presented in Fig. 2a. The $^3S_1$ states are produced directly in $e^+e^-$ annihilation. The remaining levels are observed in radiative transitions. All the levels predicted by potential models (a triplet $\chi_c$ and singlets $\eta_c$) and $\eta_c'$ are observed, with the exception of a single level $1^1P_1$ observation of which is in general rather complicated. In addition, three more quasibound states lying above the threshold for production of mesons with open charm are known.

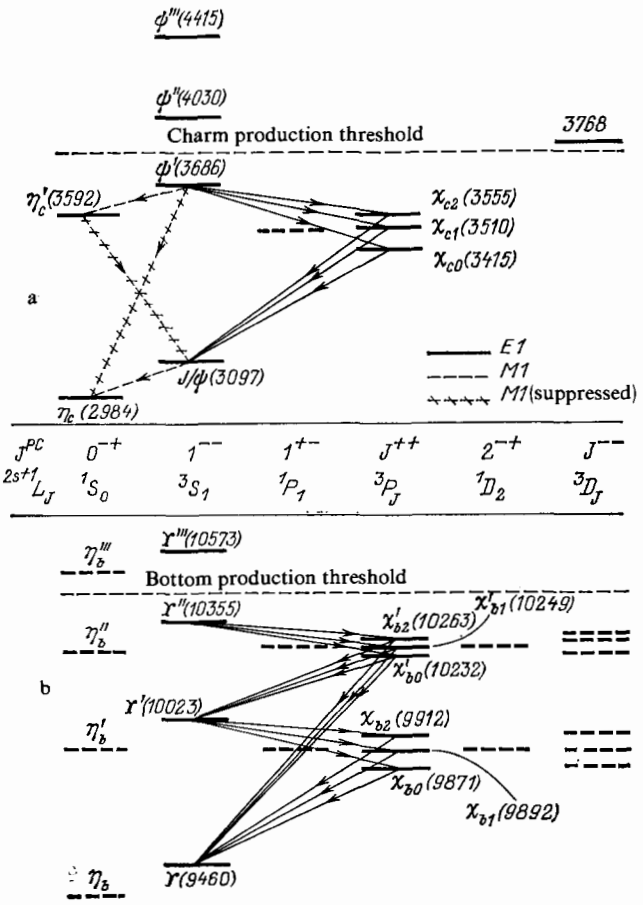


FIG. 2. Scheme of the energy levels and radiative transitions in charmonium (a) and bottomonium (b).

A new family of bottomonium, i.e., particles with the quark composition $b\bar{b}$, was first reported in 1978. Here there are already three $^3S_1$ states below the threshold for production of $B$ mesons (particles with open bottom, which have also recently been detected experimentally). They differ by the principal quantum number and are denoted by $\Upsilon$, $\Upsilon'$, and $\Upsilon''$. In addition, to them, two triplets of $^3P_J$ states ($\chi_b$ and $\chi_b'$)have been discovered in this family. The remaining states predicted by potential models have so far not been found. The scheme of the energy levels of the bottomonium family is presented in Fig. 2b. One additional level above the threshold for production of mesons with open flavor is also known.

Figure 2 shows the spectroscopic notation for the levels ($^{2s+1}L_J$ and $J^{PC}$) and the symbols ($J/\psi$, $\Upsilon$, $\Upsilon'$, etc.) for a given ground state and its radial excitations (with a given orbital angular momentum and total spin of the system), as well as the masses of the corresponding particles (in MeV). The solid lines denote the levels which have been detected experimentally, and the dashed lines indicate the levels predicted by potential models but not yet found experimentally. The arrows show the radiative transitions between different levels. The masses are usually measured with an accuracy of about a tenth of a percent. The record accuracy has been obtained in a measurement of the masses of the $\Upsilon$ mesons by the Novosibirsk group[1]: $m_\Upsilon = 9460.6 \pm 0.4$ MeV, $m_{\Upsilon'} = 10\,023.8 \pm 0.5$ MeV, and $m_{\Upsilon''} = 10\,355.5 \pm 0.5$ MeV.

The quantum numbers of the detected resonances are usually determined experimentally from the characteristic decays of these resonances. For example, cascade decays with emission of photons help to determine the total angular momentum and charge parity, and hadronic decay modes into, say, two or three pseudoscalar mesons restrict the possible values of the total angular momentum and parity of the system, and so forth.

In the schemes of Fig. 2, the fine splitting is responsible for the appearance of the triplets of levels of the $\chi_c$ and $\chi_b$, $\chi_b'$ mesons. The magnitude of the splitting is related to the strength of the spin-orbit interaction. The superfine splitting, i.e., the spin-spin interaction, manifests itself in the form of a mass difference between the $^1S_0$ and $^3S_1$ states (a mass difference between the $\eta_c$ meson and the $J/\psi$, etc.).

The top quark and, accordingly, the toponium family with the quark composition $t\bar{t}$, have so far not been detected. [*Translator's note*: It was reported in July 1984 that definite experimental evidence for the existence of the top quark had been found at CERN.] If we follow the predictions of the potential models discussed below, the spectroscopy of toponium should be much richer than for charmonium or bottomonium. For example, instead of two or three $^3S_1$ states, we have here as many as about seven or eight such subthreshold states (for a top-quark mass of order 20–40 GeV).

Information about the mesons $F$, $D$, and $B$ with open

flavor is relatively scarce. The known states are the $1^1S_0$ states of $D(1870)$ with the quark composition $u\bar{c}$, $F(2030)$ with the composition $s\bar{c}$, and $B(5270)$ with the composition $d\bar{b}$, and the $1^3S_1$ states of $D^*(2010)$, $F^*(2140)$, and $B^*(5320)$.

### 2. Decay widths

Experimental data on the properties of the decays of particles in the charmonium and bottomonium families are presented in Tables I–III.

In the Introduction we mentioned briefly the physical information which can be extracted from these data. A detailed discussion of the conclusions that have been drawn and of the results of the comparison with potential models will be given in Sec. IV.

## III. NONRELATIVISTIC POTENTIAL MODEL

### 1. Assumptions and equations

The title of this section reflects the most radical assumptions of the potential approach to the physics of heavy quarkonia.

The first assumption is that in the leading approximation heavy quarkonia can be described adequately by nonrelativistic quantum mechanics. The validity of this hypothesis is confirmed both by naive estimates of the velocities of the motion of the quarks in quarkonia according to the virial theorem[2] and by an accurate calculation of the ground-state expectation value $\langle v^2/c^2\rangle$, where $v$ is the velocity of motion of the quarks. For one of the potentials[3] which describes experiment most successfully, we have, for example, $\langle v^2/c^2\rangle_{J/\psi} = 0.23$ and $\langle v^2/c^2\rangle_{\Upsilon} = 0.08$. It is clear that for charmonium the relativistic effects can be important (but not decisive!), whereas for heavier $\Upsilon$ they are negligibly small. This naive prognosis is confirmed in the course of a detailed discussion of relativistic corrections to the various quantities in $J/\psi$ and $\Upsilon$ in Sec. V.

The second assumption is that the interaction which determines the basic properties of heavy quarkonia can be described by a local spherically symmetric potential $V(r)$, where $r$ is the distance between the quark and the antiquark in the quarkonium. The possible role of nonpotential effects (the role of the continuum and the interaction with the vacuum fields of QCD) will be discussed briefly in Sec. V. Here we note only that for a successful description of the various properties of heavy quarkonia using a local potential (including relativistic corrections if required) we are compelled to assume that nonpotential effects are in fact small.

Thus, in the nonrelativistic potential model of quarkonium, its energy spectrum and the corresponding wave functions are found from the Schrödinger equation

$$-\frac{\hbar^2}{2\mu}\nabla^2\Psi(\mathbf{r}) + [V(\mathbf{r}) - E]\Psi(\mathbf{r}) = 0, \tag{1}$$

where $\mu = m_1m_2/(m_1+m_2)$ is the reduced mass of the system formed from quarks with masses $m_1$ and $m_2$, $\mathbf{r}$ is the distance between the quarks, $V(\mathbf{r})$ is the interaction potential, $E$ is the energy eigenvalue, and $\Psi(\mathbf{r})$ is the wave function. For a centrally symmetric potential $V(r)$, Eq. (1) takes the form

$$u'' + \frac{2\mu}{\hbar^2}\left[E - V(r) - \frac{l(l+1)\hbar^2}{2\mu r^2}\right]u(r) = 0,$$
$$u(0) = 0, \quad u'(0) = R(0), \tag{2}$$

where $u(r) = rR(r)$, $R(r)$ is the radial wave function, and $l$ is the orbital quantum number. To solve (2), it remains to specify the explicit form of $V(r)$ and the value of the reduced mass $\mu$. We note at once that since the quarks are evidently not observed in the free state (quark confinement), their masses are poorly determined quantities. For the nonrelativistic problem (2), this means that $\mu$ becomes a parameter of the problem, and its numerical value can be determined by

TABLE I. Widths of the leptonic decays of charmonium and bottomonium.

| Characteristic | J/ψ | Υ |
|---|---|---|
| Γ (1S), keV | 4,6±0.4 | 1.17±0,04 |
| Γ (2S)/Γ (1S) | 0.44±0.06 | 0.45±0,08 |
| Γ (3S)/Γ (1S) | 0,16±0.02 | 0.32±0,06 |
| Γ (4S)/Γ (1S) | 0,098 | 0.24±0,05 |
| Γ (1D), keV | 0.26±0,05 | — |
| Γ (2D), keV | 0.77±0.23 | — |

TABLE II. Widths of the radiative transitions in charmonium and bottomonium.

a) Charmonium family

| | | | |
|---|---|---|---|
| BR (ψ′ → γ + χ₂) | 0.077±0,015±0,012 | Γ (ψ′ → γχ₂), keV | 17±4 |
| BR (ψ′ → γ + χ₁) | 0,088±0,005±0,014 | Γ (χ₂ → γψ), keV | 330±170 |
| BR (ψ′ → γ + χ₀) | 0.097±0,006±0,016 | Γ (ψ′ → γχ₁), keV | 19±4 |
| BR (ψ′ → γχ₂ → γγψ), % | 1,26±0,08 | Γ (χ₁ → γψ), keV | < 700 |
| BR (ψ′ → γχ₁ → γγψ), % | 2.38±0,12 | Γ (ψ′ → γχ₀), keV | 21±4 |
| BR (ψ′ → γχ₀ → γγψ), % | 0.059±0,015 | Γ (χ₀ → γψ), keV | 97±38 |
| BR (ψ′ → γη_c′), % | 0.2—1,3 (95% C.L.) | | |
| BR (ψ′ → γη_c), % | 0.29±0,08 | | |
| BR (ψ → γη_c), % | 1,20±0.53 | | |

b) Bottomonium family (see Ref. 35)

| | | | |
|---|---|---|---|
| BR (Υ′ → γΥ (1³P₂)), % | 6,1+1,4 — (CUSB)<br>5,6±1,2±1.3—(CB) | Γ (Υ′ → γΥ (1³P₂)), keV | 1,6 |
| BR (Υ′ → γΥ (1³P₁)), % | 5,9±1,4—(CUSB)<br>5,4±1,2±1,2—(CB) | Γ (Υ′ → γΥ (1³P₁)), keV | 1,6 |
| BR (Υ′ → γΥ (1³P₀)), % | 3.5±1,4—(CUSB)<br>2,9—(90% C.L) (CB) | Γ (Υ′ → γΥ (1³P₀)), keV | 1,0 |
| | | Γ (Υ″ → γΥ (2³P_J)), keV | 6,5±0.8±0.6 |

TABLE III. Total and hadronic widths of charmonium and bottomonium.

| a) Charmonium family | | | |
|---|---|---|---|
| $\Gamma_{tot}(\psi)$, MeV | $0.063\pm0.009$ | $\Gamma_{3g}(\psi)$, keV | $44\pm6$ |
| $\Gamma_{tot}(\psi')$, MeV | $0.215\pm0.040$ | $\Gamma_{3g}(\psi')$, keV | $40\pm10$ |
| $\Gamma_{tot}(\psi'')$, MeV | $25\pm3$ | BR $(\psi\to\gamma\pi^0)$ | $(3.6\pm1.1\pm0.8)\cdot10^{-5}$ |
| $\Gamma_{tot}(\psi(4030))$, MeV | $52\pm10$ | BR $(\psi\to\gamma\eta')$ | $(36\pm5)\cdot10^{-4}$ |
| $\Gamma_{tot}(\psi(4160))$, MeV | $71\pm20$ | BR $(\psi\to\gamma\eta)$ | $(8,6\pm0.9)\cdot10^{-4}$ |
| $\Gamma_{tot}(\psi(4415))$, MeV | $43\pm20$ | BR $(\psi\to\gamma f(1270))$ | $(15\pm4)\cdot10^{-4}$ |
| $\Gamma_{tot}(\eta_c')$, MeV | $<8$ (95% C.L.) | $\Gamma_{tot}(\chi_2)$, keV | $3\pm2$ |
| $\Gamma_{tot}(\eta_c)$, MeV | $12.4\pm4.6$ | $\Gamma_{tot}(\chi_1)$, keV | 2,6 |
| BR $(\psi'\to\pi^0{}^1P_1(3520\text{MeV}))$, % | $<55$ | $\Gamma_{tot}(\chi_0)$, keV | $16\pm4$ |
| **b) Bottomonium family** | | | |
| $\Gamma_{tot}(\Upsilon)$, MeV | $(3.43^{+0.78}_{-0.56})\cdot10^{-2}$ | $\Gamma_{3g}(\Upsilon)$, keV | $26,6^{+7.8}_{-5.6}$ |
| $\Gamma_{tot}(\Upsilon')$, MeV | $(2.87^{+0.56}_{-0.41})\cdot10^{-2}$ | $\Gamma_{3g}(\Upsilon')$, keV | $12,7^{+5.8}_{-4.1}$ |
| $\Gamma_{tot}(\Upsilon'')$, MeV | $(1.74\pm0,3)\cdot10^{-2}$ | $\Gamma_{3g}(\Upsilon'')$, keV | $8\pm2$ |
| $\Gamma_{tot}(\Upsilon''')$, MeV | $19.8\pm5.5\pm5$ | $\Gamma_{\gamma gg}(\Upsilon)$, keV | 1 |
| $\Gamma_{\pi\pi}(\Upsilon')$, keV | $6\pm2$ | $\Gamma_{\gamma gg}(\Upsilon')$, keV | 0.5 |
| $\Gamma_{\pi\pi}(\Upsilon'')$, keV | $1.0\pm0.5$ | $\Gamma_{\gamma gg}(\Upsilon'')$, keV | 0.3 |

requiring that the results obtained by means of Eq. (2) agree with the experimental data. There appears to be no method of independent determination of the value of $\mu$ which should occur in (2). The potential model is based on constituent quarks. If various interaction potentials are used, the quark masses can vary by as much as 10%. Typical values of the masses are $m_c \approx 1.5$ GeV and $m_b \approx 4.8$ GeV.

### 2. Choice of the interaction potential

The most important ingredient of the nonrelativistic potential program is the potential $V(r)$ describing the interaction of the quark and the antiquark in the quarkonium. The choice of this potential is not unique, in view of the absence of a consistent theory (at all distances). However, it is restricted, on the one hand, by theoretical arguments concerning the properties of the interaction of quarks and, on the other, by experimental information about quarks and quarkonia. All the potentials which are employed are phenomenological and differ from one another only in the degree of faith of their inventors in the theoretical evidence at small and large distances, in conjunction with the virtuosity of the interpolation between these limiting cases. The meaning of this game of interpolation lies in the hope that it will help to reveal the character and origin of the variation of the QCD interactions in the intermediate range of distances.

#### *a) Phenomenological potentials*

If we confine ourselves to the experimental data on the absence of quarks in the free state and on the approximate equality of the splittings between the $2^3S_1$ and $1^3S_1$ levels in charmonium (589 MeV) and bottomonium (564 MeV) (see Fig. 2), the simplest analytic potentials can be written in the logarithmic form[4)] (Quigg and Rosner[4])

$$V(r) = C_0 \ln\left(\frac{r}{r_0}\right), \tag{3}$$

where $C_0 = 733$ MeV and $r_0^2 = 1/2\mu^2$, or in the quasilogarithmic form (Martin[5])

$$V(r) = A + Br^{\alpha}, \tag{4}$$

where $A = -8064$ MeV, $B = 6870$ MeV, and $\alpha = 0.1$ (the simple formula $\lim_{\varepsilon\to0}[(r^{\varepsilon}-1)/\varepsilon] = \ln r$ is used).

#### *b) Theoretical evidence*

However, potentials which make use of certain theoretical information about the properties of the interaction of quarks are more popular. According to contemporary ideas, the interaction of quarks is described by a non-Abelian gauge theory—quantum chromodynamics (QCD). The interaction is mediated by the exchange of massless vector particles with color charge—gluons.

The specific character of QCD consists of the fact that the only consistently developed method of calculations in field theory—perturbation theory—is applicable in it only at small distances (at large momentum transfers). For very heavy quarkonia with a small bound-state radius, this means that the interaction potential is dominated by the term due to single-gluon exchange:

$$V(\mathbf{q}^2) \sim \frac{\alpha_s(q^2)}{q^2} \quad \text{or} \quad V(r) \sim \frac{\alpha_s(r)}{r}, \tag{5}$$

where $\alpha_s = g^2/4\pi$, $g$ is the constant of the color interaction, and $\mathbf{q}$ is the 3-momentum transferred between the quark and the antiquark. The weakening of the interaction at small distances manifests itself in a dependence of $\alpha_s$ on $q^2$ (or on $r$) of the type

$$\alpha_s \sim \frac{1}{\ln(q^2/\Lambda^2)} \quad (\text{for } q^2\to\infty)$$
$$\text{or} \tag{6}$$
$$\alpha_s \sim \frac{1}{\ln(1/r^2\Lambda^2)} \quad (\text{for } r\to0)$$

(here $\Lambda$ is the QCD parameter), which is obtained in a very perspicuous manner in the renormalization-group approach and determines the phenomenon of "asymptotic freedom."

In going to larger distances (smaller momentum transfers), perturbation theory ceases to be valid and it is necessary to resort to additional arguments. What is most popular here is the idea that as the quarks are separated from each

[4)]This is the only potential in which the splitting of the levels is independent of the masses of the particles.

other there is stretched in the space between them a string (a chromoelectric tube), which leads to a linear growth of the potential with increasing interquark distance. Confinement of quarks of precisely this type is obtained, for example, in a lattice theory.[6] Then

$$V(q^2) \sim \frac{1}{q^4}\,(q^2 \to 0) \quad \text{or} \quad V_l(r) \sim r_l\,(r \to \infty), \tag{7}$$

which corresponds to an interaction of the quarks with a constant force $F = -dV(r)/dr = \text{const}$.[5)] A linear growth of the potential arises also from an infrared (small $q^2$) asymptotic behavior of the gluon propagator of the form (see, for example, Ref. 7)

$$D(q^2) \sim \frac{1}{q^4}. \tag{8}$$

Naturally, besides the linearly rising term $V = kr$, the potential may also have nonleading terms in the limit of large distances. For example, the quantum fluctuations of the string[8] lead (*à la* Coulomb) to a correction to the potential at large distances:

$$V(r)|_{r\to\infty} = kr - \frac{\gamma}{r}. \tag{9}$$

Other possibilities have also been discussed (for further detail, see Eq. (40)).

We summarize the information which has been obtained:

$$\begin{cases} V(r)|_{r\to 0} \sim \dfrac{1}{r} \quad \text{or} \quad \dfrac{1}{r\ln(1/r\Lambda)}, \\ V(r)|_{r\to\infty} \sim kr. \end{cases} \tag{10}$$

These properties provide the basis for the choice of most of the potentials (in contrast to (3) and (4)). The potentials which are used differ from one another in two respects: first, they may or may not take into account the phenomenon of asymptotic freedom (the two variants in the upper line of (10)), and second, they may differ in the character of the interpolation between the two limiting regimes in (10).

In addition, all this can be done in either the coordinate or the momentum representation.

### *c) Potentials without asymptotic freedom*[6)]

We begin with the potentials which can be written down directly in the coordinate representation. The simplest interpolation from the Coulomb regime to the linearly rising behavior is given by the so-called Cornell potential[9]

$$V(r) = -\frac{a}{r} + kr, \tag{11}$$

where $a = 0.52$ and $k = 0.18$.

A more complicated interpolation, which takes into account the logarithmic character of the potential at intermediate distances (characteristic of charmonium and bottomonium), as discussed in Sec. III.2a, was proposed by Bhanot and Rudaz[10]:

$$V(r) = \begin{cases} -0{,}8/r, & r < 0{,}9; \\ 0{,}846\ln r/r_0, & 0{,}9 \leqslant r \leqslant 7{,}0; \\ 0{,}12r, & r > 7{,}0, \end{cases} \tag{12}$$

where $r_0 = 2.58$.

In the lowest approximation in $\alpha_s$, a potential of the form $a/r + kr$ is also obtained from the potential of Gupta *et al.*[11] (see Eq. (55)), which takes relativistic effects into account.

### *d. "Asymptotically free" potentials*

A modified form of the Bhanot-Rudaz potential (12) which takes into account asymptotic freedom was given by Krasemann and Ono[12]:

$$V(r) = \begin{cases} -\dfrac{8\pi}{25}\dfrac{1}{r\ln(\mu/r)} + c_1, & r < 0{,}365; \\ 0{,}69\ln\dfrac{r}{r_0}, & 0{,}365 \leqslant r \leqslant 3{,}45; \\ 0{,}156r, & r > 3{,}45, \end{cases} \tag{13}$$

where $r_0 = 1.63$, $c_1 = 0.4$, and $\mu = 2.54$. In the coordinate representation, the following potentials, written in a single analytic form, have also been used:

$$V(r) = -\frac{16\pi}{27}\frac{1}{r\ln(1/r^2\Lambda^2 e^{3c})} + V_0 - e^{-\mu r} + kr \tag{14}$$

(Richardson[13]), where $c = 0.5772$ is Euler's constant and $k$, $V_0$, $\Lambda$, and $\mu$ are constants,

$$V(r) = \frac{4}{3}\frac{\alpha_0\cdot(1-\Lambda r)^2}{r\ln(\Lambda r)} \tag{15a}$$

(Fogleman *et al.*[14]), where $\alpha_0$ and $\Lambda$ are constants, and

$$V(r) = 0{,}1768r - 1{,}093\left[r\ln\left(\frac{2{,}384\exp(-0{,}4022\cdot r)}{r} + 2{,}718\right)\right]^{-1} \tag{15b}$$

(Levine and Tomozawa[15]).

In the momentum representation, all the potentials which have been studied possess asymptotic freedom. The point is that they were written down by making direct use of the results of QCD, in which this phenomenon is automatically taken into account. The interpolation of the potential is usually made by means of an interpolation of either the coupling constant or its logarithmic derivative—the so-called Gell-Mann–Low function. If allowance is made for the single-loop corrections to the Born diagram with single-gluon exchange, we have the following expression for the potential $V(q^2)$ (Fig. 3):

$$V(q^2) = -\frac{4}{3}\frac{16\pi^2\rho(q^2)}{q^2}, \tag{16}$$

where $\rho(q^2) = \alpha_s(q^2)/4\pi$, and the factor $1/q^2$ gives the gluon propagator $D(q^2) \sim 1/q^2$. Since all the interpolations existing in the literature make use of Eq. (16), the interpolated quantity actually becomes the coupling constant, i.e., $\rho(q^2)$. Before turning to concrete interpolations, we discuss the asymptotic behavior of $\rho(q^2)$ for $q^2 \ll 1$ and $q^2 \gg 1$. For large $q^2$, QCD perturbation theory gives (see, for example,

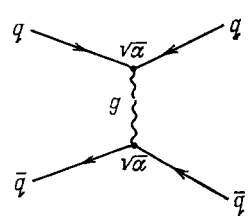


FIG. 3. Diagram with single-gluon exchange.

[5)]The simplest estimates lead to a force of 16 tons! Of course, it is not necessary to imagine that this string can become infinitely long. However, for the typical distances in quarkonia the description of confinement by means of a rising potential is justified.

[6)]The potentials and the parameters in them are given in giga-electronvolts.

Ref. 16)

$$\rho(q^2)|_{q^2\to\infty} \approx \frac{1}{b_0 \ln(q^2/\Lambda^2)} - \frac{b_1}{b_0^2}\frac{\ln\ln q^2/\Lambda^2}{(\ln q^2/\Lambda^2)^2} + \ldots, \quad (17)$$

where $b_0 = (33 - 2n_f)/3$, $b_1 = (306 - 38n_f)/3$, $n_f$ is the number of "unfrozen" quark flavors. In order to ascertain the asymptotic behavior of $\rho(q^2)$ at small $q^2$, we make use of the formula which relates the interaction potentials in the momentum and coordinate spaces:

$$V(\mathbf{r}) = \int \frac{d^3q}{(2\pi)^3} V(\mathbf{q}^2) e^{i\mathbf{q}\mathbf{r}}. \quad (18)$$

Using now Eq. (16), we obtain

$$V(r) = -\frac{32}{3}\int dq\cdot\rho(q^2)\frac{\sin qr}{qr}, \quad (19)$$

from which it can be seen that the linear growth of the potential $V(r) = kr$ as $r\to\infty$ corresponds to a coupling constant with the asymptotic behavior

$$\rho(q^2)|_{q^2\to 0} \sim \frac{1}{q^2}. \quad (20)$$

Equation (19) also helps us to reconstruct the nonleading asymptotic behaviors of $V(r)$ ($\rho(q^2)$) in the limit of large $r$ (small $q^2$) under appropriate assumptions about the behavior of $V(r)$ or $\rho(q^2)$ in this limit. Thus, for the leading asymptotic behaviors of $\rho(q^2)$ we have

$$\rho(q^2) \sim \begin{cases} 1/\ln(q^2/\Lambda^2), & q^2 \gg 1, \\ 1/q^2, & q^2 \ll 1. \end{cases} \quad (21)$$

The simplest parameter-free[7)] interpolation of $\rho(q^2)$ which takes into account the leading asymptotic behaviors of $\rho$ as $q^2\to\infty$ and $q^2\to 0$ is the Richardson interpolation[13]

$$\rho(q^2) = \frac{1}{b_0 \ln[1+(q^2/\Lambda^2)]}. \quad (22)$$

For clarity, we write down the asymptotic behaviors of (22):

$$\begin{cases} \rho(q^2)|_{q^2\to\infty} = \dfrac{1}{b_0\ln(q^2/\Lambda^2)} - \dfrac{\Lambda^2}{b_0 q^2 \ln^2(q^2/\Lambda^2)}, \\ \rho(q^2)|_{q^2\to 0} = \dfrac{\Lambda^2}{b_0 q^2}. \end{cases} \quad (23)$$

We call attention to the fact that the second term in the expression for $\rho(q^2)$ in (23) does not agree with the perturbation-theory result (17). A modification of the Richardson interpolation which allows for a possible nonleading term in the asymptotic behavior of $\rho(q^2)$ as $q^2\to 0$ was considered by Willey[17]:

$$\rho(q^2) = \left(\frac{1}{x} + Bx^\nu\right)\exp(-x^2) + \frac{1-\exp(-x^2)}{\ln(x+1)}, \quad (24)$$

where $x = Q^2/\Lambda^2$, and the asymptotic behavior of $\rho(q^2)$ as $q^2\to 0$ takes the form

$$\rho(q^2)|_{q^2\to 0} \approx \frac{\Lambda^2}{b_0}\frac{1}{q^2} + B\left(\frac{q^2}{\Lambda^2}\right)^\nu, \quad (25)$$

in which $B$ and $\nu$ are numerical coefficients. The analytic expressions for the coordinate-space potentials corresponding to (22) and (24) are very cumbersome and are therefore given in the Appendix.

The interpolation formulas for $\rho(q^2)$ become more complicated if we require that not only the main term, but also the next term of the QCD perturbation-theory expansion (see Eq. (17)) is reproduced at large $q^2$. It is much simpler in this case to interpolate the Gell-Mann–Low $\beta$ function determined by the renormalization-group equation (see, for example, Ref. 18):

$$\frac{d\rho(q^2)}{d\ln q^2} = \beta(\rho). \quad (26)$$

In the limit of small $\rho$, the $\beta$ function can be calculated by means of perturbation theory:

$$\beta(\rho)|_{\rho\to 0} \approx -b_0\rho^2 - b_1\rho^3; \quad (27)$$

the coefficients $b_0$ and $b_1$ have already appeared in Eq.(17). Naturally, the asymptotic behavior (17) is obtained from (27) and (26).

To reproduce the asymptotic behavior (20) at small $q^2$, it is necessary that

$$\beta(\rho)|_{\rho\to\infty} \sim -\rho. \quad (28)$$

The simplest algebraic interpolation between the two regimes (27) and (28) containing no free parameters was proposed by Dremin[19]:

$$\beta(\rho) = -\frac{b_0\rho^2 + (b_1+b_0^2)\rho^3}{1+b_0\rho+(b_1+b_0^2)\rho^2}. \quad (29)$$

This is one of the possible Padé approximants for $\beta(\rho)$. According to (26) and (29), the relation between $\rho$ and $q^2$ can be written in the form

$$\ln\frac{q^2}{\Lambda^2} = \frac{1}{b_0\rho} - \ln\rho + \frac{b_1}{b_0}\ln b_0 + \left(1+\frac{b_1}{b_0}\right)\ln\left[\rho\left(1+\frac{b_1+b_0^2}{b_0}\rho\right)^{-1}\right], \quad (30)$$

from which it can be seen clearly that $\Lambda^2$ is not a parameter of the interpolation, but plays the role of a constant of integration—the scale of $q^2$. This parameter of QCD is uniquely related to the slope $k$ of the linearly rising potential (see (10)), i.e., to the slope of the Regge trajectories or to the constant tension in the string. Using (30), (16), and (18), we obtain

$$\Lambda^2 = \frac{3kb_0}{8\pi}\left(1+\frac{b_1}{b_0^2}\right)^{1+(b_1/b_0^2)}. \quad (31)$$

For example, for $k = 0.2$ GeV$^2$ we have $\Lambda = 0.69$ GeV if $n_f = 4$.

A somewhat more complicated interpolation formula (Dremin and Leonidov[20]) is obtained if we require that the results reproduce not only the first two terms of the expansion at small $\rho$ and the leading asymptotic behavior at large $\rho$, but also the corrections to this asymptotic behavior due to the quantum fluctuations of the string (see (9)):

$$-\beta(\rho) = \left[\left(\frac{b_1+b_0^2}{1-\rho_g b_0}\right)\rho^3 + b_0\rho^2\right]\left[\left(\frac{b_1+b_0^2}{1-\rho_g b_0}\right)\rho^2 + \left(\frac{b_0+\rho_g b_1}{1-\rho_g b_0}\right)\rho + 1\right]^{-1}, \quad (32)$$

where $\rho_g = 1/64$.

An interpolation formula proposed by Celmaster and Henyey[21] contains a single free parameter $\rho_0$:

$$\beta(\rho) = -\frac{84\rho^2(\rho+\rho_0)}{81\rho^2+(9-64\rho_0)\rho+9\rho_0}. \quad (33)$$

Richardson's interpolation (22) given above obviously corresponds to a $\beta$ function containing an exponential function:

$$\beta(\rho) = -b_0\rho^2\left[1-\exp\left(\frac{-1}{b_0\rho}\right)\right]. \quad (34)$$

A modification of (34) which reproduces both terms of the perturbation-theory expansion for $\rho(q^2)$ in Eq. (17) was proposed by Buchmüller *et al.*[22]:

$$\beta(\rho)^{-1} = \frac{b_1\exp(-l\rho)}{b_0^2\rho} - \frac{1}{b_0\rho^2[1-\exp(-1/b_0\rho)]}, \quad (35)$$

where $l$ is a free parameter (in the calculations the authors

[7)]We assume throughout that $\Lambda^2$—the characteristic scale of $q^2$—is not a truly free parameter, but is fixed to some extent by QCD.

use the value $l = 24$).

For all the foregoing interpolations of $\beta(\rho)$ with the known values of the slopes of the Regge trajectories (or the linear part $k$ of the potential), the values of $\Lambda$ are several times larger than the scale assumed in QCD ($\Lambda_{QCD} \approx 100$–200 MeV). No unique relation between $\Lambda$ and $\Lambda_{QCD}$ has been established (see also Secs. III.3 and IV.5).

Abe *et al.*[23] attempted to obtain an interpolation in which the parameter $\Lambda$ agrees with $\Lambda_{QCD}$ by specifying a $\beta$ function which is practically identical to (35) at small and large $\rho$ and varies much more sharply in the region of intermediate values of $\rho$. In this way, the managed to reproduce the spectrum of the charmonium family rather well.

It should be noted also that calculations in the framework of lattice models[6] make it possible to reproduce the $\beta$ function at large $\rho$. However, their interpolation in the region of intermediate $\rho$ is so steep that it does not permit a description of the experimental data on quarkonia (see the next section).

Thus, summarizing, we can state that the procedure of reconstructing the potential is manifestly ambiguous, since the art of interpolation, which is readily accessible to everyone working in this field, is restricted only by the purely esthetic requirements of simplicity and the smallest possible number of free parameters. Moreover, however diverse in form the interpolation formulas are, it is found (see Sec. IV.1) that in the region of distances corresponding to the rms radii of charmonium and bottomonium they all lead to very similar potentials, but the differences between them at smaller distances (to which toponium is sensitive) do make it possible to select the best interpolation; this will undoubtedly be important for an understanding of the structure of QCD.

### 3. Theoretical basis

To what extent does quantum chromodynamics restrict the choice of the behavior of the potential at small, large, and intermediate distances? Is it in general correct to speak of the potential approach, and, if so, what are its consequences for QCD?

According to Eq. (16), the potential is related to fundamental concepts of QCD such as the coupling constant (or the renormalization-group $\beta$ function) and the gluon propagator. The appropriate asymptotic behaviors (according to perturbation theory for small $\rho$, and according to lattice and string models for large $\rho$) have been used to construct the various interpolation formulas.

However, Eq. (16) for the static potential is valid only at the single-loop level. If allowance is made for the two-loop diagrams, it is found that the static interaction potential, (i.e., the interaction energy of an infinitely heavy quark and antiquark) is given by the expression[16,24–26]

$$V(q^2) = -\frac{4}{3}\frac{16\pi^2\rho(q^2)}{q^2}\left[1 + \frac{3}{5}4\pi^2\rho(q^2)\right], \qquad (36)$$

where $\rho(q^2)$ is calculated in the corresponding approximation in the original coupling constant. This leads directly to the limit of applicability of Eq. (16). We give the simplest estimate: the correction becomes of the order of unity when $\rho^{1/2} = (1/2\pi)(5/3)^{1/2} \approx 0.2$, i.e., roughly when $b_1\rho \sim b_0$. Thus, the use of Eqs. (16), (17), and (27) is self-consistent at small $\rho$.

With regard to the scale of variation of $q^2$ (or $r$) given by the parameter $\Lambda$, it may be noted that this parameter is different in the momentum and coordinate representations and is distinct from $\Lambda_{QCD}$. Thus, the parameter $\Lambda$ in the expression for the coupling constant $\rho(q^2)$ which enters into the static potential (16) is related to $\Lambda_{QCD}$ by the equation[22,25]

$$\ln\frac{\Lambda_M}{\Lambda_{QCD}} = \frac{1}{2b_0}\left(\frac{124}{27} - \frac{10}{19}n_f\right) \qquad (37)$$

(where $\Lambda_{QCD} \equiv \Lambda_{\overline{MS}}$), i.e., in the momentum representation the parameter $\Lambda_M$ exceeds $\Lambda_{QCD}$ by a factor of about 1.65. At the same time, the parameter $\Lambda$ which appears in the formulas for the potential in coordinate space exceeds $\Lambda_M$ by a factor of about 1.78, since[27]

$$\Lambda_K = e^c\Lambda_M, \qquad (38)$$

where $c = 0.5772$ is Euler's constant. Equations (37) and (38) may be useful for a detailed test of the QCD interaction potential in superheavy quarkonia (for example, in toponium).

In general, when we go over to smaller $q^2$, even the parameter $\Lambda$ may change from a constant into a weakly varying function of $q^2$. Thus, when allowance is made for the finite values of the quark masses, the discontinuities in Eq. (37) at the thresholds for production of new flavors are replaced by a smoother dependence which takes into account the threshold effects. We shall not give here the corresponding formulas, referring the reader to the original papers.[28] Here we mention only an attempt[29] to take into account threshold effects in a potential model, in which it was proposed to replace $n_f$ in the formula for $\rho(q^2)$ by

$$f(q^2) = \sum_{i=1}^{n_f}\frac{q^2}{q^2+m_i^2}. \qquad (39)$$

Inclusion of threshold effects is important for precision spectroscopy of quarkonia, since it leads to noticeable, though not very large, corrections. These corrections in fact indicate the accuracy claimed by the calculations which have been made.

At small distances in the limit of weak coupling, all the effects appear to be well controlled, and the breakdown of the perturbation-theory expansion for the various quantities with increasing coupling constant occurs in a self-consistent manner. The situation is much more complicated in the case of the asymptotic behavior in the strong-coupling region. Asymptotic freedom disappears with increasing distance not only because of the growth of the coupling constant, but also on account of nonperturbative power corrections due to vacuum fluctuations.[30] The interaction resulting from the long-wave fluctuations has a nonpotential character.[31] At the same time, it was shown in Ref. 32a that inclusion of short-wave vacuum fluctuations (instantons with dimensions smaller than a certain cutoff radius) leads to the appearance of an additional local interaction potential and thus does not alter the potential character of the interaction at the distances typical of heavy quarkonia. This picture can be realized, for example, in the model of the QCD vacuum proposed in Ref. 32b. The role of the short-wave fluctuations was considered also in Ref. 32c. Thus, the success of potential models in describing charmonium and bottomonium (see the next section) evidently indicates that asymptotic free-

dom breaks down with increasing distance primarily because of the short-wave (and not the long-wave) fluctuations of the vacuum.

This breakdown manifests itself precisely in the region of interpolated distances in the phenomenological potentials. As we have already mentioned, the asymptotic behavior at large distances does not in itself have a profound meaning. Nevertheless, it should be noted that the linear growth of the potential with distance is confirmed by the following facts: 1) an infrared asymptotic behavior of the gluon propagator[7] of the form $1/q^4$ is consistent with the Schwinger-Dyson equations; 2) in field theory on a lattice,[6] the integral over a Wilson loop is proportional to its area; 3) in the various formulas for the action of a string used in the papers of Ref. 33, identical expressions were obtained for the static potential.

$$V(r)=\sqrt{\frac{r^2}{(2\pi\alpha')^2}-\frac{1}{12\alpha'}}, \tag{40}$$

and at large $r$ these lead to a formula of the type (9).

## IV. COMPARISON OF THE NONRELATIVISTIC POTENTIAL MODEL WITH EXPERIMENT

### 1. Comparison of the interaction potentials

The diversity of the potentials described in the preceding section is deceptive—in the range of distances $0.1\text{F}\leqslant r\leqslant 1$ F characteristic of charmonium and bottomonium, they approach one another so closely that it was practically impossible to distinguish them in Fig. 4, in which they were combined into a single line. This is understandable—indeed, we have represented here only those potentials which to some extent (but nevertheless rather successfully) describe the experimental data on these families. Nonetheless, it is important to consider not only the value of the potential, but also its derivatives, and therefore there is a difference between the various potentials even in this region of distances. This difference becomes much greater on going to the distances characteristic of toponium (in Fig. 4 we have marked the radius of toponium for the assumed mass 70 GeV), since here there is already a clearly visible difference between the behaviors of the various potentials. This is the reason for the importance of data on toponium, which will make it possible to distinguish the most correct potential.

One might think that the potential at small distances

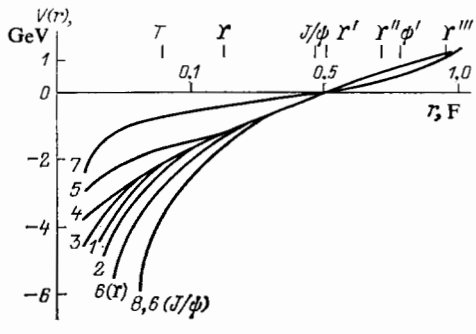


FIG. 4. Interaction potential between the quarks as a function of $r$. Curves: 1) from Ref. 3; 2) Ref. 36; 3) Ref. 15; 4) Ref. 12; 5) Ref. 5; 6) Ref. 9; 7) Ref. 6; 8) Ref. 10. Along the horizontal axis we have indicated the characteristic distances for the members of the families of charmonium, bottomonium, and toponium (for a $T(1^3S_1)$ mass of about 70 GeV).

could be reconstructed by means of the method of the inverse scattering problem, using data on charmonium and bottomonium. Unfortunately, an attempt to do this[34] led to a band of predictions in the region of toponium which coincides precisely with that shown in Fig. 4 and which varies from the deepest Cornell potential (6) to the smoothest Martin potential (5).

In the nonrelativistic approach, the potential does not depend on the energy or on the quark flavor. At the same time, the relativistic corrections are different for quarks of different flavors; in addition, for the high-lying levels there are different couplings to the open decay channels. These effects will be discussed when we make a comparison with the experimental data and given estimates of the corresponding corrections.

### 2. Energy spectrum

The nonrelativistic potential model is capable of predicting only the centroids of the levels. Naturally, this model cannot claim to describe the fine and superfine splittings, which we shall consider in the next section. In Tables IV and V we give the energy spectra of charmonium and bottomonium, calculated with the most characteristic potentials (see Fig. 4), as well as the experimental values of the masses of the levels.

In general, it should be noted that the values of the quantum numbers of the levels are usually assigned first in accordance with calculations based on potential models and are then, as a rule, justified by experiment.

It can be seen from Table IV that the spectroscopy of charmonium is described quite well by all the potentials, and the agreement becomes even better if relativistic corrections are taken into account (see Sec. V).[8)] In the case of bottomonium, the relativistic corrections are very small, so that the results given in Table V are changed only slightly. It should be noted here that doubt is cast on the Cornell potential and the Martin potential—the two extreme potentials in Fig. 4. The first of them requires a flavor dependence of the coefficient $a$ in the Coulomb term ($a_\Upsilon = 0.48$ GeV$^2$). The second, being very slowly varying, predicted excessively low values for the positions of the $1^3P_J$ $\Upsilon$ levels at 9861 MeV. Recent data of the groups CUSB, Crystal Ball, and CLEO (Ref. 35) give for the centroid the value $9901 \pm 3$ MeV, which is in good agreement with the predictions of other potentials[3,11,12,36] and differs appreciably from the value $M(1^3P_J) = 9830 \pm 30$ MeV obtained using nonrelativistic sum rules (see, for example, Ref. 37). The values closest to the experimental masses of the $1^3P_J$ levels are given by the potentials reconstructed by means of the interpolations of the $\beta$ functions given in (32) and (35).

### 3. Leptonic widths

In Tables VI and VII we give the leptonic widths of the $S$ levels of charmonium and bottomonium. The width for

[8)]The relativistic corrections usually reduce somewhat the mass of the centroid of a system of levels. (In particular, the centroids of the $^3S_1$ and $^3P_J$ levels come closer together.[48,57]) Of course, the splitting of the levels is given solely by the relativistic effects.

TABLE IV. Spectrum of the charmonium family predicted by potential models, and comparison with the experimental data (in GeV).

| State | a) | b) | c) | d) | e) | f) | g) | Experiment |
|---|---|---|---|---|---|---|---|---|
| $1^1S_0$ | 3,095 | 3,095 | 3,100 | 3,001 | 3,000 | 2,981 | 3,01 | 2,984 |
| $1^3S_1$ | 3,095 | 3,095 | 3,100 | 3,100 | 3,100 | 3,097 | 3,10 | 3,097 |
| $1^3P_2$ | 3,522 | 3,502 | 3,510 | 3,553 | 3,540 | 3,561 | 3,56 | 3,555 |
| $1^3P_1$ | 3,522 | 3,502 | 3,500 | 3,502 | 3,500 | 3,515 | 3,50 | 3,510 |
| $1^3P_0$ | 3,522 | 3,502 | 3,520 | 3,419 | 3,420 | 3,416 | 3,40 | 3,415 |
| $1^1P_1$ | 3,522 | 3,502 | 3,520 | 3,521 | — | 3,531 | — | — |
| $2^1S_0$ | 3,684 | 3,687 | 3,70 | 3,635 | 3,670 | 3,600 | — | 3,592 |
| $2^3S_1$ | 3,684 | 3,687 | 3,70 | 3,700 | 3,690 | 3,685 | — | 3,684 |

a) Cornell group[9]; b) Martin[5]; c) Willey[17]; d) Buchmüller and Tye[3]; e) Henriques *et al.*[45]; f) Gupta *et al.*[11]; g) sum rules.[53]

decay of a heavy vector resonance into a lepton pair is described in the nonrelativistic approximation by the Van Royen–Weisskopf formula[38]

$$\Gamma^{(0)}(V \to l^+l^-) = 4\alpha^2 e_q^2 |R_V(0)|^2 M_Y^{-2}, \tag{41}$$

from which it can be seen that this width is determined by the quark charge $e_q$, the resonance mass $M_Y$, and the probability that the quark and antiquark meet at a single point, i.e., the wave function at $r = 0$. The radiative chromodynamical corrections to this formula are also known[39]:

$$\Gamma = \Gamma^{(0)}\left(1 - \frac{16}{3\pi}\alpha_s\right). \tag{42}$$

The data in Tables VI and VII demonstrate, first, the correctness of the values of the electric charges ascribed to the $c$ and $b$ quarks, since they do not allow the discrepancies of a factor of 4 which would occur with other assignments. At the same time, if radiative corrections are not included, the leptonic widths of the S levels of charmonium are about twice as large as the experimental values, and those of the S levels of bottomonium are larger by a factor of 1.5. Inclusion of corrections according to (42) improves the situation, although the result cannot be regarded as completely reliable, both because of the possible role of higher corrections in $\alpha_s$ and because of the uncertainties in the estimate of $\alpha_s$. Moreover, kinematic corrections may also be important.[3]

In the ratios of the widths, which are usually in good agreement with experiment, all the corrections cancel. With regard to the absolute values, there is qualitative agreement. It should be noted that the ratio of the widths of the $2S$ and $1S$ levels, for example, gives directly the ratio of the corresponding squares of the wave functions, which according to experiment is less than unity, thus indicating that the potential has a convex form (i.e., $V''(r) < 0$).[40]

### 4. Radiative transitions

The widths of the electric dipole $E1$ transitions can be calculated according to the formulas

$$\Gamma(n^3S_1 \xrightarrow{\gamma} n'^3P_J) = \frac{4}{3}\alpha\omega^3 e_q^2 \frac{(2J+1)}{9} M_{nn'}^2, \tag{43}$$

$$\Gamma(n^3P_J \xrightarrow{\gamma} n'^3S_1) = \frac{4}{9}\alpha\omega^3 e_q^2 M_{nn'}^2, \tag{44}$$

where

$$M_{nn'} = \int_0^\infty dr r^3 R_n R_{n'} \tag{45}$$

is the dipole matrix element, $\omega$ is the frequency of the transition, $e_q$ is the quark charge, and $R$ are the radial wave functions. Here again we have confirmation of the assignment for

TABLE V. Spectrum of the bottomonium family predicted by potential models, and comparison with the experimental data (in GeV).

| State | a) | b) | c) | d) | e) | f) | g) | Experiment |
|---|---|---|---|---|---|---|---|---|
| $1^1S_0$ | 9,459 | 9,46 | 9,46 | 9,414 | 9,427 | 9,43 | 9,46 | — |
| $1^3S_1$ | 9,459 | 9,46 | 9,46 | 9,46 | 9,462 | 9,46 | 9,46 | 9,459 |
| $1^3P_2$ | 9,96 | 9,861 | 9,91 | 9,880 | 9,910 | 9,83 | 9,93 | 9,911 |
| $1^3P_1$ | 9,96 | 9,861 | 9,91 | 9,849 | 9,893 | 9,83 | 9,93 | 9,891 |
| $1^3P_0$ | 9,96 | 9,861 | 9,91 | 9,808 | 9,868 | 9,83 | 9,93 | 9,870 |
| $1^1P_1$ | 9,96 | 9,861 | 9,91 | 9,862 | 9,900 | 9,83 | 9,93 | — |
| $2^1S_0$ | 10,1040 | 10,025 | 10,02 | 9,997 | 9,994 | — | 10,02 | — |
| $2^3S_1$ | 10,4040 | 10,025 | 10,02 | 10,02 | 10,013 | — | 10,02 | 10,023 |
| $2^3P_2$ | 10,31 | 10,242 | 10,25 | 10,236 | 10,266 | — | 10,28 | 10,263 |
| $2^3P_1$ | 10,31 | 10,242 | 10,25 | 10,212 | 10,252 | — | 10,28 | 10,249 |
| $2^3P_0$ | 10,31 | 10,242 | 10,25 | 10,180 | 10,232 | — | 10,28 | 10,232 |
| $2^1P_1$ | 10,31 | 10,242 | 10,25 | 10,222 | 10,258 | — | 10,28 | — |
| $3^1S_0$ | 10,395 | 10,36 | 10,35 | 10,332 | 10,339 | — | 10,47 | — |
| $3^3S_1$ | 10,395 | 10,36 | 10,35 | 10,85 | 10,355 | — | 10,47 | 10,355 |

a) Cornell group[9]; b) Martin[5]; c) Bykov, Dremin, and Leonidov[36]; d) Buchmüller and Tye[3]; e) Gupta *et al.*[11]; f) sum rules[37]; g) potential reconstructed from the $\beta$ function on a lattice.[6]

TABLE VI. Widths of the leptonic decays of charmonium calculated in potential models, and comparison with the experimental data.

| State | a) | b) | c) | d) | e) | f) | g) | Experiment |
|---|---|---|---|---|---|---|---|---|
| Γ (1S), keV | 4.8 | — | — | 3.70 | 4.3 | 5.07 | 4.3 | 4.8±0.6 |
| Γ (2S)/Γ (1S) | 0.43 | 0.40 | 0.46 | 0.46 | 0.3 | 0.50 | | 0.44±0.06 |
| Γ (3S)/Γ (1S) | 0.30 | 0.25 | — | 0.32 | — | — | | 0.16±0.02 |
| Γ (4S)/Γ (1S) | 0.23 | — | — | 0.25 | — | — | | 0.098 |

a) Cornell group[9]; b) Martin[5]; c) Willey[17]; d) Buchmüller and Tye[3]; e) Henriques *et al.*[45]; f) Gupta *et al.*[11]; g) sum rules.[53]

the electric charge $e_q$ of the quark. What is more significant is that the radiative transitions permit a detailed study of the properties of the wave functions of quarkonia at large distances (see (45)) and a rather accurate determination of the spectrum of the emitted photons (the quantity $\omega^3$ appears in (43) and (44), so that the radiative widths are very sensitive to the error in $\omega$). The widths of different transitions also react differently to changes in the wave functions. For example, in the transition $2S \to 1P + \gamma$, because $R_2$ is of variable sign, there are strong cancellations in the integral (45), so that small changes in $R_1$ and $R_2$ are very noticeable in the quantity $M_{nn'}$. On the other hand, the transition $1P \to 1S + \gamma$ is insensitive to changes in $R_1$, since there are no cancellations in (45) (the function $R_1$ is of definite sign). In general, the widths of $E$ 1 transitions are sensitive to the relative positions of the maxima and the nodes of the wave functions, so that they control the wave functions locally (and not in an integrated sense, as for the leptonic widths).

The results give in Table VIII show that the widths of the $E$ 1 transitions in charmonium are about twice as large as the experimental values even for the potential models which work fairly successfully. At the same time, as can be seen from Table IX, the situation is much better for the $E$ 1 transitions in bottomonium. This can be explained by the fact that in the sense of charmonium there are large relativistic corrections (see Sec. V), whose inclusion makes it possible to restore agreement with experiment.

### 5. Total and hadronic widths

Quarkonia decay into hadrons through channels which are forbidden by the OZI rule. In a nonrelativistic treatment, the quark and antiquark must meet at a single point and annihilate into two (for $^1S_0$ states) or three (for $^3S_1$ states) gluons, which are then converted into the final hadrons with probability unity.[9)] Accordingly, the hadronic widths of such decays are proportional to the square or the cube of the strong interaction constant $\alpha_s$ and to the square of the modulus of the wave function at zero distance, i.e.,

$$\Gamma(V \to gg \to h) = \frac{8}{3}\alpha_s^2 |R_\eta(0)|^2 M_\eta^{-2}, \tag{46}$$

$$\Gamma(V \to ggg \to h) = \frac{40(\pi^2-9)}{81\pi}\alpha_s^3 |R_V(0)|^2 M_V^{-2}. \tag{47}$$

These formulas differ from the corresponding formulas for parapositronium and orthopositronium only by the substitutions for the masses, the replacement of $\alpha$ by $\alpha_s$, and the numerical factors due to the averaging over the quark color.

The results of calculations of the hadronic widths of quarkonia and their experimental values are presented in Table X. By combining the data on the hadronic and leptonic widths of quarkonia in the nonrelativistic approximation, it is possible to determine the value of the strong-interaction constant $\alpha_s$ which determines the quark-gluon vertex: $\alpha_s(J/\psi) = 0.19 \pm 0.01$ and $\alpha_s(\Upsilon) = 0.16 \pm 0.01$, in agreement with other estimates.

Various experimentally measurable relations between the widths of two- and three-gluon decays of quarkonia and a number of other quantities containing $\Gamma_{\gamma gg}$, $\Gamma_{eg}$, and $\Gamma_{2g}$ make it possible to test the predictions of QCD for the radiative corrections to these characteristics (see Ref. 60).

It should be recalled that a consistent study of the hadronic widths in potential models is possible only if a renormalization-group analysis of the potential is made. In this case, the constant $\alpha_s$ is reproduced by the model automati-

TABLE VII. Widths of the leptonic decays of bottomonium calculated in potential models, and comparison with the experimental data.

| State | a) | b) | c) | d) | e) | f) | g) | Experiment |
|---|---|---|---|---|---|---|---|---|
| Γ (1S), keV | 1.25 | 0.58 | 1.13 | 1.07±0.24 | 1.29 | 1.15±0.2 | 0.31 | 1.17±0.04 |
| Γ (2S)/Γ (1S) | 0.36 | 0.51 | 0.42 | 0.44 | 0.48 | — | 0.88 | 0.45±0.08 |
| Γ (3S)/Γ (1S) | 0.25 | 0.35 | 0.30 | 0.32 | 0.35 | — | 0.79 | 0.32±0.06 |
| Γ (4S)/Γ (1S) | 0.20 | 0.27 | 0.26 | 0.26 | — | — | 0.72 | 0.24±0.05 |

a) Cornell group[9]; b) Martin[5]; c) Bykov, Dremin, and Leonidov[36]; d) Buchmüller and Tye[3]; e) Gupta *et al.*[11]; f) sum rules[37]; g) "lattice" potential.[36]

[9)]This method of calculating decay probabilities is called the Appelquist-Politzer prescription (for a detailed discussion of its applicability and of its breakdown in the decays of the $\eta_c$ and $\chi_0$ mesons, see the review of Ref. 60).

TABLE VIII. Widths of the radiative $E1$ transitions in charmonium calculated in potential models, and comparison with the experimental data.

| Transition, keV | a) | b) | c) | d) | e) | Experiment |
|---|---|---|---|---|---|---|
| $2^3S_1 \to 1^3P_J$ | 124,2 | 145 | 116,4 | 57 | 70 | 57±8 |
| $2^3S_1 \to 1^3P_2$ | 28,9 | 38 | 30,0 | 14 | 31 | 17±5 |
| $2^3S_1 \to 1^3P_1$ | 45,3 | 49 | 40,8 | 21 | 31 | 19±5 |
| $2^3S_1 \to 1^3P_0$ | 50,0 | 58 | 45,6 | 22 | 8 | 21±6 |
| $1^3P_J \to 1^3S_1$ | 828 | 1059 | 730 | 745 | 404 | — |
| $1^3P_2 \to 1^3S_1$ | 398 | 496 | 340 | 367 | 136 | 330±170 |
| $1^3P_1 \to 1^3S_1$ | 289 | 381 | 260 | 258 | 160 | <700 |
| $1^3P_0 \to 1^3S_1$ | 141 | 182 | 130 | 120 | 108 | 97±38 |

a) Cornell group[9]; b) Buchmüller and Tye[3]; c) Krasemann (variant with the Klein-Gordon equation)[41]; d) Henriques *et al.*[45]; e) sum rules.[54]

cally, and not introduced into it from without. Unfortunately, the majority of models based on the $\beta$ function[3,36] do not make it possible to obtain better agreement between the theoretical estimates of the hadronic widths and the experimental data because of the excessively large values of the parameter $\Lambda$. It seems to us that the situation can be resolved by introducing into the model a scalar confining potential. The slope $k_V$ of the linearly rising Lorentz-vector part of the potential is related to the parameter $\Lambda$ by the equation $\Lambda^2 = C(n_f)k_V$, where $C(n_f)$ is a coefficient depending on the number $n_f$ of "unfrozen" flavors. By choosing the confining potential in the form of a superposition of Lorentz-scalar ($k_S r$) and Lorentz-vector ($k_V r$) components, $V \sim k_S r + k_V r$, of which the first is dominant (the value of $k_V$ is small), the value of $\Lambda$ an be reduced to a level which makes it possible to reproduce the hadronic widths.

### 6. Predictions for toponium

The toponium family consists of the bound states of the hypothetical superheavy t quark and its antiquark. In many respects, this system will be more convenient for studying the nature of the quark-antiquark interaction than charmonium and bottomonium. This is the case, first, because of the very small relativistic corrections for toponium (so that the use of naive nonrelativistic models for its description should yield good results), and second, because of the large number of bound states and the great diversity of transitions between them, which ensure rich experimental information about these systems. In addition to the information provided by charmonium and bottomonium about the potential of the quark-antiquark interaction in the range 0.2 F$\leqslant r \leqslant$1 F, toponium will make it possible to study the behavior of the potential at even smaller distances $r \lesssim 0.1$ F, where the asymptotically free behavior of the effective coupling constant $\alpha_s$ leads to important experimentally observable consequences. Thus, toponium will be the first bound state whose characteristics permit direct verification of the asymptotically free behavior of the effective coupling consant at small distances. It can be seen from Tables XI–XIII, in which we give the various characteristics of the members of the $T$ family, what large differences exist between the predictions of the properties of toponium obtained using potentials which take into account the phenomenon of asymptotic freedom and using potentials which do not. (The numbers are given for the case in which the mass of the $1S$ level is 70 GeV. More detailed information for various masses is contained in Ref. 36.) It can be seen from Tables XI–XIII that the first experimental data on toponium will make it possible to distinguish "asymptotically free" potentials from potentials which do not take this property into account. This requires quite low

TABLE IX. Widths of the radiative $E1$ transitions in bottomonium calculated in potential models, and comparison with the experimental data.

| Transition, keV | a) | b) | c) | d) | Experiment |
|---|---|---|---|---|---|
| $3^3S_1 \to 2^3P_2$ | 2,5 | 4,25 | 3,6 | 1,8 | |
| $3^3S_1 \to 2^3P_1$ | 1,5 } =4,5 | 2,55 } =7,65 | 2,17 } =6,5 | 1,9 } =5,0 | 6,5±0,8±0,6 |
| $3^3S_1 \to 2^3P_0$ | 0,5 | 0,85 | 0,72 | 1,3 | |
| $2^3P_2 \to 2^3S_1$ | 17 | 15,9 | | 17 | |
| $2^3P_1 \to 2^3S_1$ | 17 | 15,9 | | 16 | |
| $2^3P_0 \to 2^3S_1$ | 17 | 15,9 | | 12 | |
| $2^3S_1 \to 1^3P_2$ | 1,35 | 3,43 | | 0,96 | ~ 1,6 |
| $2^3S_1 \to 1^3P_1$ | 0,81 } =2,43 | 2,06 } =6,18 | | 1,01 } =2,75 | ~ 1,6 } ≈ 4,2 |
| $2^3S_1 \to 1^3P_0$ | 0,27 | 0,69 | | 0,78 | ~ 1,0 |
| $1^3S_2 \to 1^3S_1$ | 36 | 34,5 | | 39 | |
| $1^3P_1 \to 1^3S_1$ | 36 | 34,5 | | 36 | |
| $1^3P_0 \to 1^3S_1$ | 36 | 34,5 | | 26 | |

a) Cornell group[9]; b)Buchmüller and Tye[3]; c) Bykov, Dremin, and Leonidov[36]; d) Silverman.[56]

TABLE X. Widths of the hadronic decays of bottomonium calculated in potential models, and comparison with the experimental data (in keV).

| Characteristic | Ref. 9 | Calculation using Eq. (32) | Experiment |
|---|---|---|---|
| $\Gamma_{tot}(\Upsilon)$ | 21 | | $34.3^{+7.8}_{-5.6}$ |
| $\Gamma_{3g}(\Upsilon)$ | 12 | 91 | $26.6^{+7.8}_{-5.6}$ |
| $\Gamma_{\gamma gg}(\Upsilon)$ | 0,3 | | 1 |
| $\Gamma_{tot}(\Upsilon')$ | 18 | | $28.7^{+5.6}_{-4.1}$ |
| $\Gamma_{3g}(\Upsilon')$ | 4,3 | 36 | $12.7^{+5.8}_{-4.1}$ |
| $\Gamma_{\gamma gg}(\Upsilon')$ | 0,1 | | 0.5 |
| $\Gamma_{tot}(\Upsilon'')$ | 11 | | $17.4\mp3$ |
| $\Gamma_{3g}(\Upsilon'')$ | 3,0 | 17 | $8\mp2$ |
| $\Gamma_{\gamma gg}(\Upsilon'')$ | 0,1 | | 0.3 |

accuracies of the experimental data: ~500 Mev for the determination of the energy levels, and ~2 keV for the determination of the leptonic widths. We note that numerical similarity of the potentials dos not by itself imply similarity of all the characteristics calculated on their basis. Evidently, the leptonic and photon widths are the characteristics which are most sensitive to the details of the behavior of the potentials, and it is these that should be used to choose the potential describing the interaction of the heavy quark and antiquark in the bound state.

## V. ROLE OF RELATIVISTIC CORRECTIONS AND POSSIBLE NONPOTENTIAL EFFECTS

### 1. Relativistic corrections

Allowance for relativistic effects is one of the most important problems of the physics of heavy quarkonia. The study of these effects not only helps to establish the limits of applicability of the nonrelativistic potential model and permits calculations of the (sometimes very important) relativistic corrections, but also makes it possible to look at the nature of the confining forces in a new light. The experimental data on the energy spectrum of heavy quarkonia clearly indicate the existence of relativistic interactions depending on the quark spins, which are absent in the nonrelativistic potential picture. In the families of charmonium and bottomonium, there are observed experimentally (in the radiative $E1$ transitions $N^3S_1 \xrightarrow{\gamma} N - 1^3P_J \xrightarrow{\gamma} N - 1^3S_1^{35}$) triplets of $^3P_J$ states with a characteristic splitting of the order of tens of MeV. The members of a triplet differ from one another by the value of the total angular momentum $J$, and therefore it is natural to assume that the splitting can be attributed to the spin-orbit interaction $H \sim \mathbf{L}\cdot\mathbf{S}$, where $\mathbf{L}$ is the orbital angular momentum of the quark-antiquark pair and $\mathbf{S}$ is its total spin (the fine structure). In this way, they are described by potential models with allowance for relativistic corrections. In the charmonium family, experiments also reveal radiative $M1$ transitions between orthoquarkonium ($^3S_1$) and paraquarkonium ($^1S_0$). It is natural to assume that the corresponding splitting can be attributed to the spin-spin interaction $H \sim \mathbf{S}_1\cdot\mathbf{S}_2$, where $\mathbf{S}_1$ and $\mathbf{S}_2$ are the spins of the quark and the antiquark (the hyperfine structure).

There exist also kinematic corrections due to the motion of the quarks with respect to their overall center of mass. This type of correction may evidently be revealed in the study of the photon and leptonic widths of heavy quarkonia.

In the theoretical analysis of the relativistic corrections, the results depend strongly on the assumptions concerning the nature of the confining forces included in the model. Thus, by comparing theoretical estimates with experimental data, one can attempt to understand the structure of the spin-spin and spin-orbit interactions and study the Lorentz structure of the confining part of the interquark potential. For instance, if there is a Lorentz-scalar interaction potential $V_m$, then the fine splitting of the levels changes by an amount proportional to the derivative $V'_m$ (for further details, see below).

The study of relativistic corrections not only makes it possible to understand the nature of the spin interactions and the confining forces in QCD, but also removes many difficulties which arise when the potential model of quar-

TABLE XI. Mass of the the $1S$ state* and mass splitting** in the toponium family for various potentials ($m_t = 35$ GeV) (in GeV).

| State | Ref. 3 | Ref. 36 | Ref. 15 | Ref. 12 | Ref. 5 | Ref. 9 |
|---|---|---|---|---|---|---|
| 1S | 68.771 | 69.162 | 68,757 | 69.156 | 68.475 | 64,419 |
| 2S | 0.805 | 1,064 | 0,763 | 0,626 | 0,523 | 4,233 |
| 3S | 1.142 | 1,467 | 1.094 | 0.949 | 0,828 | 5,071 |
| 4S | 1.290 | 1,707 | 1,325 | 1,175 | 1,056 | 5.421 |
| 1P | 0.711 | 0,950 | 0,676 | 0.527 | 0,377 | 4,225 |
| 2P | 1,078 | 1.395 | 1.030 | 0.879 | 0,726 | 5,064 |
| 3P | 1.412 | 1,659 | 1.269 | 1.116 | 0,970 | 5.413 |
| 4P | 1.676 | 1.859 | 1.481 | 1.325 | 1.181 | 5.633 |
| 1D | 1,008 | 1.322 | 0.957 | 0.833 | — | 5.046 |
| 2D | 1.254 | 1.603 | 1.304 | 1.046 | 0.890 | 5.396 |
| 3D | 1.525 | 1.806 | 1.411 | 1.303 | 1.101 | 5.613 |
| 4D | 1.817 | 2.015 | 1.636 | 1.412 | 1.328 | 5.819 |

*First row.
**Second and subsequent rows.

TABLE XII. Leptonic widths of the $1S$–$4S$ levels of toponium for various potentials.

| State | $m_t = 35$ GeV | | | | | |
|---|---|---|---|---|---|---|
| | Ref. 3 | Ref. 36 | Ref. 15 | Ref. 12 | Ref. 5 | Ref. 9 |
| Γ (1S), keV | 6,091 (6,94) | 10,095 (11,61) | 4,937 (5,63) | 3,300 (3,80) | 0,898 (1,02) | 164,02 (178,78) |
| Γ (2S)/Γ (1S) | 0,29 | 0,26 | 0,29 | 0,39 | 0,54 | 0,11 |
| Γ (3S)/Γ (1S) | 0,17 | 0,14 | 0,18 | 0,24 | 0,35 | 0,04 |
| Γ (4S)/Γ (1S) | 0,12 | 0,11 | 0,14 | 0,20 | 0,36 | 0,02 |
| The numbers in parentheses allow for the $Z^0$-boson decay channel. | | | | | | |

konia is compared with experiment.[10)] For example, the width of an $E1$ transition for a nonrelativistic system of a bound quark and antiquark is described by Eq. (43) and is determined by an overlap integral over the wave functions of the initial and final states. The value of this integral depends on the relative positions of the nodes and maxima of the wave functions, and in this sense $E1$ transitions permit a "local" test of how correctly they are reproduced in the framework of any particular model. (We recall that the leptonic widths $\Gamma_{ee} \sim |\Psi(0)|^2$ control the wave functions only at a single point). In "naive" potential models (those which do not include relativistic corrections), the widths obained for the photon transitions in the charmonium family are systematically too large by a factor 2–4. By using the Klein-Gordon equation and the Dirac equation[41] to calculate the wave functions which appear in the overlap integral (see Eq. (45)), it has been possible to reduce significantly this discrepancy between theory and experiment (see Table VIII).

It seems to us that although the Klein-Gordon and Dirac equations contain no information about the spin-spin interactions (the source of the field external to the test particle is assumed to be infinitely heavy and spinless), they take into account correctly the influence of the kinematic corrections; this is reflected in the change of the widths of the $E1$ transitions in heavy quarkonia toward the experimental values. Evidence for this is provided by the values calculated in Ref. 36 for the $E1$ transitions in the bottomonium family. The $\Upsilon$ particles, which consist of the heavier (in comparison with the $c$ quark) $b$ quark and $\bar{b}$ antiquark, are much more nonrelativistic than in the $J/\Psi$ (and, thus, the kinematic corrections in bottomonium are much smaller than in charmonium). Therefore it is to be expected that the results of "naive" potential models for bottomonium will correspond better to experiment. Indeed, we have, for example, the experimental value $\Gamma_{E_1}(3^3S_1 \to 2^3P_J + \gamma) = 6.5 \pm 0.8 \pm 0.6$ keV,[35] whereas the calculations of Ref. 36 give $\Gamma_{E_1}(3^3S_1 \to 2^3P_J + \gamma) = 6.5$ keV! A consistent treatment of relativistic corrections to the widths of $E1$ transitions[42] leads to agreement between the theoretical and experimental results for the charmonium family as well.

The main theoretical tools for the study of relativistic corrections to the potential model are the Bethe-Salpeter and Breit-Fermi equations, to whose description we now turn.

The most general relativistic equation for bound states is the Bethe-Salpeter equations[43,44] (Fig. 5).

$$J_{ab}(x_1, x_2) = \int d^4x_3\, d^4x_4\, d^4x_5\, d^5x_6 S_F'^a(x_1 - x_3)\, S_F'^b(x_2 - x_4)\, G_{ab}(x_3, x_4, x_5, x_6) \cdot J_{ab}(x_5, x_6), \tag{48}$$

where $a$ and $b$ are indices denoting the quark and antiquark, respectively, $J_{ab}$ is the amplitude for production of a bound state by the quark $a$ and antiquark $b$ (their propagators are $S_F'^a$ and $S_F'^b$), and $G_{ab}$ is the two-particle-irreducible kernel of the Bethe-Salpeter equation describing the quark-antiquark interaction which leads to production of the bound state.

In order to obtain the Salpeter equation used in applications, we must:

a) transform to the momentum representation in (48);
b) transform to the center-of-mass system of the quark and the antiquark;

TABLE XIII. Widths of the radiative $E1$ transitions between certain levels of toponium for various potentials ($m_t = 35$ GeV).

| Transition, keV | Ref. 3 | Ref. 36 | Ref. 15 | Ref. 12 | Ref. 5 | Ref. 9 |
|---|---|---|---|---|---|---|
| 3S → 2P | 3,22 | 3,12 | 1,36 | 1,93 | 4,70 | 0,001 |
| 2P → 2S | 7,66 | 19,39 | 2,98 | 5,71 | 2,58 | 11,36 |
| 2S → 1P | 2,13 | 2,36 | 1,11 | 1,68 | 4,98 | 0,0003 |
| 1P → 1S | 8,14 | 20,12 | 12,63 | 8,57 | 5,09 | 262,60 |

[10)]It should be noted again that in general the appearance of "new" interactions is usually associated with new parameters and assumptions (for example, about the relative weights of the Lorentz scalar and the Lorentz vector in the potential—see also the discussion after Eq. (60)). However, the number of such parameters is much smaller than the number of experimental facts which can be described by means of them.

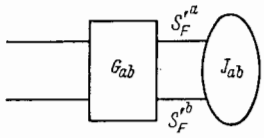


FIG. 5. Graphical representation of the Bethe-Salpeter equation.

c) assume an instantaneous interaction.

As a result, we find the Salpeter equation

$$\widetilde{\Psi}_{ab}(\mathbf{q}) = \left(\frac{\Lambda_a^+\Lambda_b^+}{E-E_a-E_b} - \frac{\Lambda_a^-\Lambda_b^-}{E-E_a+E_b}\right)\gamma_0^a\gamma_0^b\cdot 2\pi i \int d^3k\widetilde{G}_{ab}(-k^2)\,\widetilde{\Psi}_{ab}(\mathbf{q}+\mathbf{k}), \tag{49}$$

where the tildes over $\Psi$ and $G$ reflect the transition to an instantaneous, $\Lambda^{\pm}$ are the standard projection operators onto the positive- and negative-energy states, $\gamma_0$ is the Dirac matrix, $E$ is the energy of the bound state, and $E_a$ and $E_b$ are the quark and antiquark energies. In order to study the spectroscopy of quarkonia, it now remains to describe the quark-antiquark interaction (to specify the kernel $G$ or, equivalently, the interaction potential $V(r)$). Equation (49) without the second term (this omission is justified for $|E-E_a-E_b| \ll |E+E_a+E_b|$) was applied for the first time to the study of charmonium spectroscopy in Ref. 45. In Ref. 45 use was made of a potential of the form

$$V(r) = \left(\lambda r - \frac{\alpha_s}{r}\gamma_\mu^a\gamma^{b\mu} - c\right)e^{-\varkappa r} + c'(1-e^{-\varkappa r}), \tag{50}$$

where $\lambda$, $c$, $c'$, and $\varkappa$ are parameters of the problem and $\alpha_s$ is the dimensionless coupling constant of QCD. This potential is not confining, but if the parameter $\varkappa$ is small, then the levels are quite deep and, as a consequence, this case differs little from the case of a linearly rising potential.[11)]

The Salpeter equation (49) has been used also to calculate relativistic corrections to leptonic widths.[46] In the nonrelativistic limit, the expressions obtained for the leptonic widths reduce to (41).

The most popular method of calculating the leading relativistic corrections to the energy spectrum of quarkonia is the use of an interaction Hamiltonian similar to the well-kown Breit-Fermi Hamiltonian in electrodynamics[43]:

$$H = H_0 + H_{\mathrm{BF}}, \tag{51}$$

where $H_0$ is the initial nonrelativistic Hamiltonian and $H_{BF}$ is the Breit-Fermi Hamiltonian. The corrections to the nonrelativistic energy spectrum are usually calculated according to perturbation theory, where the role of the perturbing Hamiltonian is played by $H_{BF}$. From the point of view of the nonrelativistic potential model, the most consistent method of deriving $H_{BF}$ is to go over to the nonrelativistic limit in the Bethe-Salpeter equation (48) or in the Salpeter equation (49). The transition to the nonrelativistic limit is usually based on the fact that in the leading approximation the kernel of the Salpeter equation (49) is given by single-gluon exchange, improved by the renormalization-group technique. A Lorentz-scalar interaction potential is also included phenomenologically in the kernel, so that

$$\widetilde{G} \sim V_{\mathrm{V}}(\mathbf{q}^2)\,\gamma_\mu\gamma^\mu + V_{\mathrm{m}}(\mathbf{q}^2)\,I, \tag{52}$$

where $\gamma_\mu$ are the usual Dirac matrices and $I$ is the $4\times 4$ unit matrix. After the transition to the nonrelativistic limit, it is found that the Hamiltonian is given by an expression of the form

$$H = H_0 + H_{\mathrm{SD}} + H_{\mathrm{SI}}, \tag{53}$$

where $H_0$ is the initial nonrelativistic Hamiltonian, $H_{SD}$ is the part of the Breit-Fermi Hamiltonian which depends on the spins of the quarks, and $H_{SI}$ is its spin-independent part. The overwhelming majority of authors drop the third term in (53) and work with $H_{SD}$ alone. This term corresponds to the kernel (52) and can be written in the form $(m = m_q = m_{\bar{q}})$[12)]

$$\begin{aligned} H_{\mathrm{SD}} = {} & \frac{1}{2m^2r}\left(3\frac{dV_{\mathrm{V}}}{dr} - \frac{dV_m}{dr}\right)\mathbf{LS} \\ & + \frac{1}{3m^2}\left(\frac{1}{r}\frac{dV_{\mathrm{V}}}{dr} - \frac{d^2V_{\mathrm{V}}}{dr^2}\right)(3(\mathbf{s}_1\mathbf{n})(\mathbf{s}_2\mathbf{n}) - \mathbf{s}_1\mathbf{s}_2) \\ & + \frac{2}{3m^2}\Delta V_{\mathrm{V}}\cdot(\mathbf{s}_1\mathbf{s}_2), \end{aligned} \tag{54}$$

where $m$ is the quark (antiquark) mass and $\mathbf{n}$ is the unit radius vector.

It can be seen that $V_m$ changes the fine structure of the levels but does not affect the spin-spin and tensor interactions. The Hamiltonian (54) has been used by many authors.[47] Allowance was made for the spin-independent interactions (i.e., the term $H_{SI}$ in (53)) in Ref. 48. Of course, an exact calculation of $H_{SD}$ in chromodynamics is possible only in the framework of perturbation theory. In Ref. 11 a perturbation-theory interaction potential was calculated with accuracy up to the terms $O(\rho^4)$:

$$H = 2m + \frac{\mathbf{p}^2}{m} - \frac{\mathbf{p}^4}{4m^3} + V_{\mathrm{p}}(r) + V_{\mathrm{c}}(r), \tag{55}$$

where

$$\begin{aligned} V_{\mathrm{p}}(r) = {} & -\frac{4}{3}\frac{\alpha_s}{r}\left[1 - \frac{3\alpha_s}{2\pi} + \frac{\alpha_s}{6\pi}(33-2n_f)[\ln(\mu r)+c]\right] \\ & + \frac{4\alpha_s}{3m^2r}\left\{1 - \frac{3\alpha_s}{2\pi} + \frac{\alpha_s}{6\pi}(33-2n_f)[\ln(\mu r)+c]\right\}\cdot\nabla^2 \\ & + \frac{8\pi\alpha_s}{3m^2}\left\{\left[1 - \frac{3\alpha_s}{2\pi}\right]\delta(r) - \frac{\alpha_s}{24\pi^2}\right. \\ & \left.\times(33-2n_f)\nabla^2\left[\frac{\ln(\mu r)+c}{r}\right]\right\} \\ & - \frac{14\alpha_s^2}{9mr^2} + \frac{32\pi\alpha_s}{9m^2}\mathbf{s}_1\mathbf{s}_2\left\{\left[1 - \frac{\alpha_s}{12\pi}(26+9\ln 2)\delta(r)\right.\right. \\ & - \frac{\alpha_s}{24\pi^2}(33-2n_f)\nabla^2\left[\frac{\ln(\mu r)+c}{r}\right] \\ & \left.\left. + \frac{21\alpha_s}{16\pi^2}\nabla^2\left[\frac{\ln(mr)+c}{r}\right]\right]\right\} \\ & + \frac{4\alpha_s}{m^2}\left(\frac{(\mathbf{s}_1\mathbf{r})(\mathbf{s}_2\mathbf{r})}{r^3} - \frac{1}{3}\frac{\mathbf{s}_1\mathbf{s}_2}{r}\right)\left\{1 + \frac{4\alpha_s}{3\pi}\right. \\ & + \frac{\alpha_s}{6\pi}(33-2n_f)\left[\ln(\mu r)+c-\frac{4}{3}\right] \\ & \left. - \frac{3\alpha_s}{\pi}\left[\ln(mr)+c-\frac{4}{3}\right]\right\} \\ & + \frac{2\alpha_s}{m^2}\frac{\mathbf{LS}}{r^3}\left[1 - \frac{11\alpha_s}{18\pi} + \frac{\alpha_s}{6\pi}(33-2n_f)[\ln(\mu r)\right. \\ & \left. + c - 1] - \frac{2\alpha_s}{\pi}[\ln(mr)+c-1]\right]. \end{aligned}$$

The complete Hamiltonian can be written in the form

[11)]The authors of Ref. 45 were not able to solve Eq. (49) without introducing the exponential suppression in (50).

[12)]In the L·S term the coefficient 3 in front of $dV_V/dr$ occurs because the Breit-Fermi equation is written for two particles with spin, whereas the Dirac equation (in which the coefficient of $dV_V/dr$ is 1) describes the motion of a single particle with spin in the field of a spinless source.

$$H = 2m + \frac{\mathbf{p}^2}{m} - \frac{\mathbf{p}^4}{4m^3} + V_{\mathrm{p}}(\mathbf{r}) + V_{\mathrm{c}}(\mathbf{r}), \tag{56}$$

where

$$V_{\mathrm{c}}(r) = Ar - \frac{A}{2m^2}\frac{\mathbf{LS}}{r} + C; \tag{57}$$

here $\mu$, $C$, and $A$ are parameters, $c$ is Euler's constant, and $m$ is the quark (antiquark) mass. It is obvious from a comparison with (57) that a Lorentz-scalar confining potential was used in Ref. 11.

The results of calculations with this Hamiltonian are presented in Tables IV–VIII. It should be noted that this Hamiltonian does not exhaust all the versions encountered in the literature (see, for example, Ref. 47). The ambiguities which exist here (the signs in front of the various terms, the coefficients, etc.) reflect the fact that theoreticians have no unique methods for treating the nature of the confining part of the interquark potential and dividing it into Lorentz-scalar and Lorentz-vector parts. We note, however, that both in Eq. (49) and in the Hamiltonian (51), which leads to good agreement with experiment, the confining part of the potential was assumed to have a Lorentz-scalar character.

The problem of the Lorentz structure of the confining potential is intimately related to the need to introduce a dynamical quark mass (depending on the distance between the quark and the antiquark) in the application to the study of quarkonia by means of the Dirac equation.[49]

Let us consider the corresponding interaction Hamiltonian:

$$H = \boldsymbol{\alpha}\mathbf{p} + \beta m(r) + V_{\mathrm{V}}(r), \tag{58}$$

where $m(r) = m_0 + V_m(r)$ and $m_0 = \mathrm{const}$ is the mass of the "free" particle (or $m_0 = m(r_0)$ and $V_m(r_0) = 0$). The system of equations for the wave function has the form

$$\begin{aligned} &F' + \frac{\varkappa}{r}F - [\varepsilon + m_0 + V_{\mathrm{m}}(r) - V_{\mathrm{V}}(r)]\,G = 0, \\ &G' - \frac{\varkappa}{r}G + [\varepsilon - m_0 - V_{\mathrm{m}}(r) - V_{\mathrm{V}}(r)]\,F = 0, \end{aligned} \tag{59}$$

where $F$ and $G$ are the upper and lower spinors, respectively, $\varepsilon$ is the total energy, and

$$\varkappa = \begin{cases} l, & j = l - (1/2), \\ -(l+1), & j = l + (1/2) \end{cases}$$

($j$ and $l$ are the total orbital angular momenta, respectively). In the nonrelativistic limit, the system of equations (59) reduces to the ordinary Schrödinger equation with the interaction potential

$$V(r) = V_{\mathrm{V}}(r) + V_{\mathrm{m}}(r). \tag{60}$$

In the nonrelativistic problem, it makes no difference which of the terms in (60) ensures confinement of the quarks. However, an analysis of the system (59) shows directly that the appropriately normalized wave functions are obtained only when $V_m(r) \gtrsim V_V(r)$ for $r \to \infty$. Therefore the absence of an instability in the potential problem (59) is achieved only with a quark mass which grows with the distance (in general, such a growth of the mass dominates over the growth of the Lorentz-vector contribution). This corresponds to the notion of a transition from current quarks (with small mass) to constituent quarks (with large mass) as the momentum transfer drecreases (or the distance increases). An important consequence of the appearance of a dynamical quark mass is the proportionality of the fine splitting to the difference of derivatives $V'_m - V'_V$, which can be studied by comparing the theoretical results with the experimentally observed quantities. It was first noted in Ref. 50 that there are no bound states in a potential which grows linearly with the interquark distance and which is the zeroth component of a Lorentz vector in the Dirac equation. We have already in our earlier discussion of the Bethe-Salpeter and Breit-Fermi equations mentioned the need to introduce a Lorentz-scalar confining potential. Analogous statements were made previously in Ref. 51. The introduction of a Lorentz-scalar interaction potential leads to agreement between the theoretical and experimental widths of the $M1$ transitions in quarkonia.[52,57] On the basis of the experimental data, it is not possible at present to exclude completely the possibility that the confining potential contains a part which is the zeroth component of a four-vector. It seems to us most probable that the confining potential is a sum of Lorentz-scalar and Lorentz-vector parts in definite proportions. A definitive clarification of this question would require a more detailed study of the fine structure of the spectrum of heavy quarkonia.[13)]

### 2. Nonpotential effects

The relativistic corrections discussed so far were in essence derived from QCD perturbation theory (with the exception of the assumptions about the confining part of the interquark potential). There exist, however, corrections not taken into account by perturbation theory and due to the nontrivial structure of the QCD vacuum. The first type of correction is due to the long-wave fluctuations of the gluon vacuum and can be expressed in terms of the nonzero vacuum expectation values.

$$\left\langle 0 \left| \frac{\alpha_s}{\pi} G^a_{\mu\nu} G^{\mu\nu a} \right| 0 \right\rangle \approx 0{,}012\ \mathrm{GeV}^4.$$

These corrections were first estimated in Ref. 30c and have been exploited successfully since then in the most diverse applications. One such application is the calculation in the dipole approximation of corrections to the spectrum and widths of heavy quarkonia due to the long-wave fluctuations.[37] What was in fact considered here was a Coulomb system in an external chaotically oriented chromoelectric field. It was shown that such corrections cannot be adsorbed into the local static potential of the quark-antiquark interaction.[31] However, in systems consisting of a heavy quark and an antiquark, the long-wave fluctuations may be nonleading nonperturbative corrections, and the major role may be played by fluctuations of small dimensions like those considered in the model of an instanton fluid.[32b] An indication of this can be seen in the underestimation of the mass of the $1^3\mathrm{P}_J$ state in bottomonium. Inclusion of only the long-wave fluctuations leads to the value $M(1^3\mathrm{P}_J) = 9830 \pm 30$ MeV, whereas experiment gives $M(1^3\mathrm{P}_J) = 9900$ MeV. Allowance for short-wave fluctuations leads to a modification of the potential at small distances[32a]:

[13)]For example, the predictions obtained in Ref. 57 for the fine splitting of the $1^3\mathrm{P}_J$ levels of bottomonium exceed the experimentally measured values by a factor of more than 1.5. Agreement can be achieved by altering the contribution of the Lorentz scalar.

$$\Delta V(r) \sim r^2 \int \frac{d\rho}{\rho^2} D(\rho) + O(r^4),$$

where the integration is carried out over the dimensions of the instanton, and $D(\rho)$ is the density of instantons with given $\rho$. Thus, the fluctuations of the gluon vacuum may lead to dominant effects which are adsorbed into the local static potential and to small nonpotential effects due, for example, to instantons of large dimensions.

We believe that the question of the validity of the potential approach in the framework of the QCD has not yet been resolved definitively and requires a more detailed theoretical analysis. This is due to both the successes of potential models in describing the spectroscopy of quarkonium and the lack of success of nonrelativistic sum rules in describing the mass of the $1P$ level.[37] In particular, it would be of interest to investigate, in the framework of the approach proposed in Ref. 37, quarkonia with a more realistic interaction potential than the Coulomb potential. Another important nonpotential effect is the inclusion of continuum effects, i.e., the possible screening of the interaction of a heavy quark and antiquark as a result of the production of a light quark-antiquark pair (rupture of a string). Allowance for this effect naturally requires the solution of a multichannel problem.[9] An attempt at a field-theoretical treatment of this effect was made in Ref. 55. The results of these studies show that inclusion of the coupling to the continuum is important for the charmonium family. Thus, for the shifts of the levels it is found that $\Delta M(J/\psi) = -48$ MeV, $\Delta M(\psi') = -118$ MeV, and $\Delta M(\chi_J) = -90$ MeV; for the photon transitions $\Gamma_{E1}(\psi' \to \chi_0) = 43.2$ keV, $\Gamma_{E1}(\psi' \to \chi_1) = 34$ keV, and $\Gamma_{E1}(\psi' \to \chi_2) = 23$ keV, whereas when no allowance is made for the coupling to the continuum we have, respectively, $\Gamma_{E1}(\psi' \to \chi_J) = (50, 45, 29)$ keV. We note that inclusion of the continuum effects brings the theoretical values closer to the experimental data and leads to various shifts of the levels of charmonium. For bottomonium these effects should be smaller, since its low-lying states are separated from the threshold for production of $B$ mesons by a large energy interval.

Thus, the question of the role of nonpotential effects is a quantitative problem. The potential approach is suitable as long as the nonpotential corrections are small.

## VI. CONCLUSIONS

It can be seen from our discussion that the potential model is a powerful tool for studying the work of heavy quarkonia, emerging as a rather reliable guide for experiments and posing important and interesting problems for theoreticians. It has great predictive power and makes it possible to investigate with high accuracy the most diverse characteristics of the bound states of a heavy quark and an antiquark. Moreover, the potential model provides considerable information about the structure of the spin-spin and spin-orbit interactions in QCD, the effects of confinement, the coupling to the continuum, the nontrivial structure of the vacuum, etc. In addition, the model is simple from the mathematical standpoint, which is of no small importance in carrying out practical calculations. If, as most theoreticians hope, the sixth superheavy $t$ quark and its bound state with the $\bar{t}$ antiquark—toponium—are discovered in the near future, the potential model will help us to study this superheavy quarkonium and to reveal the specific character of the color interactions at small distances. It turns out that some of the existing difficulties in potential models which we described earlier open up, as they are overcome, interesting prospects for the study of fundamental effects of the theory of the strong interactions. This applies also to the study of hadronic widths and to the elucidation of the role of the long-wave and short-wave vacuum fluctuations, which are "hot" points in QCD. The situation here is not yet completely certain and requires careful and thorough study. What seems correct today may tomorrow be subject to critical analysis and radically altered, and it seems to us that the potential model is not deprived of the possibility of participating in this process.

## APPENDIX

Here we give the formulas for the potentials reconstructed on the basis of Eqs. (22) and (24).

The potential of Ref. 17 has the form

$$V(r) = \frac{\Lambda}{6\pi b_0}\rho + \overline{V}(r),$$

where

$$\overline{V}(r) = -\frac{2}{3\pi^2}\frac{\Lambda I(\rho)}{b_0\rho}, \quad \rho = \Lambda \cdot r$$

$$I(\rho) = \int_0^\infty \frac{\sin \rho y}{y} B y^{2\nu} \exp(-y^4) + \left\{\left[\frac{1}{\ln(1+y^2)} - \frac{1}{y^2}\right]\left[1 - \exp(-y^4)\right]\right\} dy.$$

The Richardson potential in the coordinate representation has the form[13]

$$V(r) = \frac{8\pi}{33 - 2n_f}\Lambda \times \left(\Lambda \cdot r - \left[1 - 4\int_1^\infty \frac{dq}{q}\exp(-q\Lambda r)/(\ln^2(q^2-1)+\pi^2)\right]\Big/\Lambda r\right).$$


[1] A. S. Astamanov *et al.*, Preprint 83-84, Institute of Nuclear Physics, Siberian Division, USSR Academy of Sciences, Novosibirsk (1983).
[2] E. D. Bloom, Preprint SLAC-PUB-3015 (1982).
[3] W. Buchmüller and S.-H. H. Tye, Phys. Rev. D **24**, 132 (1981).
[4] C. Quigg and J. L. Rosner, Phys. Rep. **56**, 167 (1979).
[5] A. Martin, Phys. Lett. **B100**, 4511 (1981).
[6] M. Bander, Phys. Rep. **75**, 205 (1981).
[7] M. Baker, Acta Phys. Pol. **B12**, 3 (1981). S. Mandelstam, Phys. Rev. D **20**, 322 (1979).
[8] M. Lüsher, Nucl. Phys. **B180**, 317 (1981).
[9] E. Eichten *et al.*, Phys. Rev. Lett. **34**, 369 (1975); Phys. Rev. D **17**, 3090 (1978); **21**, 203 (1980).
[10] A. Bhanot and K. Rudaz, Phys. Lett. **B78**, 119 (1978).
[11] S. N. Gupta *et al.*, Phys. Rev. D **26**, 3305 (1982).
[12] K. Krasemann and S. Ono, Nucl. Phys **B154**, 283 (1978).
[13] J. L. Richardson, Phys. Lett. **B82**, 272 (1979).
[14] G. Fogleman *et al.*, Lett. Nuovo Cimento **26**, 369 (1979).
[15] R. Levine and J. Tomozawa, Phys. Rev. D **19**, 1572 (1979); **21**, 840 (1980).
[16] S. Davis and F. L. Feinberg, Phys. Lett. **B78**, 90 (1978).
[17] R. S. Willey, Phys. Rev. D **26**, 3254 (1982).
[18] E. Reya, Phys. Rep. **69**, 195 (1981).
[19] I. M. Dremin, Kratk. Soobshch. Fiz. No. 1 (1982).
[20] I. M. Dremin and A. V. Leonidov, Teor. Mat. Fiz. **51**, 178 (1982).
[21] W. Celmaster and F. S. Henyey, Phys. Rev. D **18**, 1688 (1978).
[22] W. Buchmüller *et al.*, Phys. Rev. Lett. **45**, 103 (1980).
[23] V. Abe *et al.*, Phys. Rev. D **27**, 675 (1983).
[24] T. Appelquist *et al.*, Phys. Lett. **B69**, 231 (1977); Phys. Rev. D **17**, 2074 (1978).
[25] W. Fischer, Nucl. Phys. **B129**, 157 (1977).

[26]F. L. Feinberg, Phys. Rev. Lett. **39**, 316 (1976); Phys. Rev. D **17**, 2659 (1978).
[27]W. Celmaster *et al.*, Phys. Rev. D **17**, 879 (1978).
[28]C. Rosenzweig, Z. Phys. C **10**, 178 (1982). D. V. Shirkov, Preprint E2-81-274, JINR, Dubna (1981).
[29]D. B. Lichtenberg and J. G. Wills, Lett. Nuovo Cimento **32**, 86 (1981).
[30]a) A. Belavin *et al.*, Phys. Lett. **B59**, 85 (1975). b) C. Callan *et al.*, Phys. Rev. D **19**, 1826 (1979). c) M. Shifman *et al.*, Nucl. Phys. **B147**, 385, 448 (1979).
[31]M. B. Voloshin, Nucl. Phys. **B154**, 365 (1979).
[32]a) C. Callan *et al.*, Phys. Rev. D **18**, 4684 (1978). b) É. V. Shuryak, Preprint 81-118, Institute of Nuclear Physics, Siberian Division, USSR Academy of Sciences, Novosibirsk (1981). c) V. N. Baier and Yu. F. Pinelis, Preprints 82-115, 83-62, Institute of Nuclear Physics, Siberian Division, USSR Academy of Sciences, Novosibirsk.
[33]O. Alvarez, Phys. Rev. D **24**, 440 (1981). J. F. Arvis, Phys. Lett. **B127**, 106 (1983).
[34]K. J. Miller and M. G. Olsson, Phys. Rev. D **25**, 2382 (1982).
[35]See, for example: K. Han *et al.*, Phys. Rev. Lett. **49**, 1612 (1982).
[36]A. A. Bykov, I. M. Dremin, and A. V. Leonidov, Preprint No. 52, P. N. Lebedev Physics Institute, USSR Academy of Sciences, Moscow (1983).
[37]M. B. Voloshin, Preprint ITEP-30, Institute of Theoretical and Experimental Physics, Moscow (1981).
[38]V. Van Royen and W. Weisskopf, Nuovo Cimento **50**, 617 (1967).
[39]R. Barbieri, Phys. Lett. **B57**, 455 (1975).
[40]A. Martin, Phys. Lett. **B70**, 192 (1977).
[41]H. Krasemann, Preprint TH 3011, CERN (1980).
[42]K. J. Sebastian, Phys. Rev. D **26**, 2295 (1982).
[43]V. B. Berestetskiĭ, E. M. Lifshits, and L. P. Pitaevskiĭ, Kvantovaya élektrodinamika, Nauka, Moscow (1979), p. 606 [Engl. Transl., Quantum Electrodynamics, Pergamon Press, Oxford (1982)].
[44]D. Flamm and F. Schoberl, Introduction to the Quark Model of Elementary Particles, Vol. 1, Gordon and Breach, London (1982).
[45]A. Henriques *et al.*, Phys. Lett. **B64**, 85 (1976).
[46]L. Bergström *et al.*, Z. Phys. C **4**, 215 (1980). W. J. Keung and Z. J. Muzinich, Phys. Rev. D **27**, 1518 (1983).
[47]J. Rafelski and R. D. Violler, Preprint TH2673, CERN (1979).
[48]D. Beavis *et al.*, Phys. Rev. D **20**, 2345 (1979).
[49]I. M. Dremin and A. V. Leonidov, Pis'ma Zh. Eksp. Teor. Fiz. **37**, 617 (1983) [JETP Lett. **37**, 738 (1983)].
[50]M. S. Plesset, Phys. Rev. **41**, 278 (1932).
[51]M. E. Rose, Phys. Rev. **82**, 470 (1951). Ch. Long and D. Robson, Phys. Rev. D **27**, 644 (1983).
[52]G. Hardekopf and J. Sucher, Phys. Rev. D **25**, 2939 (1982). H. Grotch and K. J. Sebastian, Phys. Rev. D **25**, 2944 (1982).
[53]R. A. Bertelmann, Nucl. Phys. **B204**, 387 (1982).
[54]A. Khodjamirian, Preprint EFI-427(34)-80 (1980).
[55]E. C. Poggio and H. J. Schnitzer, Phys. Rev. D **19**, 1557 (1979).
[56]A. Silverman, in: Proc. of the 1981 Intern. Symposium on Lepton and Photon Interaction at High Energies, Bonn, August 1981 (ed. W. Pfeil), Universität Bonn (1981), p. 163.
[57]R. McClary and N. Byers, Preprint UCLA/TEP/83/12 (1983).
[58]A. I. Vaĭnshteĭn *et al.*, Usp. Fiz. Nauk **123**, 217 (1977) [Sov. Phys. Usp. **20**, 796 (1977)].
[59]B. Richter, Les Prix Nobel en 1976, Stockholm, 1977, pp. 42–47 [Russ. Transl. Usp. Fiz. Nauk **125**, 201 (1978)]. S. C. C. Ting, Les Prix Nobel en 1976, Stockholm, 1977, pp. 76–106 [Russ. Transl., Usp. Fiz. Nauk **125**, 227 (1978)].
[60]V. A. Khoze and M. A. Shifman, Usp. Fiz. Nauk **140**, 3 (1983) [Sov. Phys. Usp. **26**, 387 (1983)].
[61]A. I. Vaĭnshteĭn *et al.*, Usp. Fiz. Nauk **131**, 537 (1980) [Sov. Phys. Usp. **23**, 429 (1980)].
[62]E. D. Bloom and G. J. Feldman, Sci. Am. **246**, No. 5, 66 (1982) [Russ. Transl., Usp. Fiz. Nauk **139**, 529 (1983)].
[63]T. Appelquist, N. M. Barnet, and K. D. Lane, Ann. Rev. Nucl. Part. Sci. **28**, 387 (1978).
[64]M. Krammer and H. Krasemann, Acta Phys. Austriaca Suppl. **21**, 259 (1979).

Translated by N. M. Queen